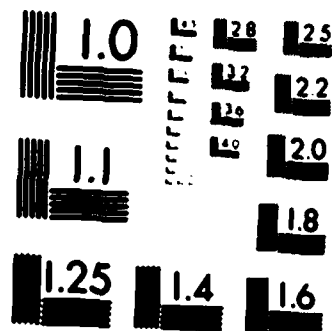END
FILMED

DTIC

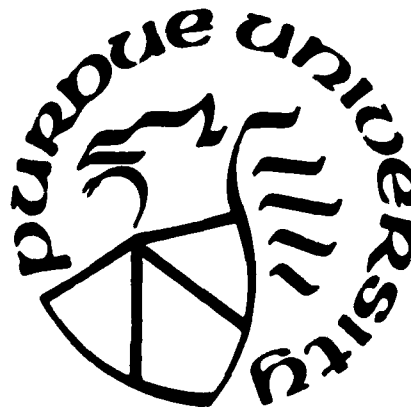MICROCOPY RESOLUTION TEST CHART
NATIONAL BUREAU OF STANDARDS-1963-A

AFOSR-TR. 85-0064

AD-A151 799

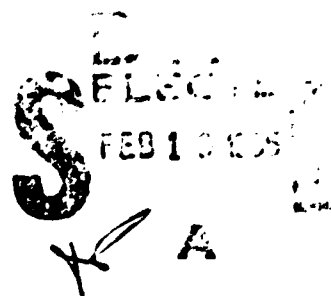# PURDUE UNIVERSITY
SCHOOL OF AERONAUTICS AND ASTRONAUTICS

Initiation, Growth, and
Coalescence of Small
Fatigue Cracks

SELECTE
FEB 1 3 1985

West Lafayette, Indiana 47907

REPORT DOCUMENTATION PAGE

1a REPORT SECURITY CLASSIFICATION	1b RESTRICTIVE MARKINGS
UNCLASSIFIED	
2a SECURITY CLASSIFICATION AUTHORITY	3 DISTRIBUTION/AVAILABILITY OF REPORT
	Approved for Public Release:
2b DECLASSIFICATION/DOWNGRADING SCHEDULE	Distribution is Unlimited.
4 PERFORMING ORGANIZATION REPORT NUMBER(S)	5 MONITORING ORGANIZATION REPORT NUMBER(S)
	AFOSR-TR- 85-0064

6a NAME OF PERFORMING ORGANIZATION	6b OFFICE SYMBOL (If applicable)	7a NAME OF MONITORING ORGANIZATION
Purdue University		AFOSR/NA
6c ADDRESS (City, State and ZIP Code)		7b ADDRESS (City, State and ZIP Code)
School of Aeronautics and Astronautics Grissom Hall West Lafayette, IN 47907		Bolling AFB DC. 20332

8a NAME OF FUNDING/SPONSORING ORGANIZATION	8b OFFICE SYMBOL (If applicable)	9 PROCUREMENT INSTRUMENT IDENTIFICATION NUMBER
Air Force Office of Scientific Research	/NA	AFOSR 82-0041

8c ADDRESS (City, State and ZIP Code)	10 SOURCE OF FUNDING NOS			
AFOSR/NA Bolling Air Force Base, D.C. 20332-6448	PROGRAM ELEMENT NO	PROJECT NO	TASK NO	WORK UNIT NO
	61102F	2307	B2	

11 TITLE (Include Security Classification)
Initiation, Growth and Coalescence of Small Fatigue Cracks

12 PERSONAL AUTHOR(S)
A.F. Grandt, Jr.

13a TYPE OF REPORT	13b TIME COVERED	14 DATE OF REPORT (Yr., Mo., Day)	15 PAGE COUNT
Annual	FROM 1/15/83 TO 1/14/84	May 1984	

16 SUPPLEMENTARY NOTATION

17 COSATI CODES			18 SUBJECT TERMS (Continue on reverse if necessary and identify by block number)
FIELD	GROUP	SUB GR	

19 ABSTRACT (Continue on reverse if necessary and identify by block number)

This interim report summarizes the second year's progress on a research effort directed at studying the initiation, growth, and coalescence of small fatigue cracks at notches. A fracture mechanics based model is described to predict the growth and coalescence of multiple cracks located at notches. The predictive model is compared with experimental results obtained with multiply cracked specimens made from a transparent polymer and for metal specimens. Current efforts and future goals are also briefly described.

20 DISTRIBUTION/AVAILABILITY OF ABSTRACT	21 ABSTRACT SECURITY CLASSIFICATION
UNCLASSIFIED/UNLIMITED ☒ SAME AS RPT ☐ DTIC USERS ☐	UNCLASSIFIED

22a NAME OF RESPONSIBLE INDIVIDUAL	22b TELEPHONE NUMBER (Include Area Code)	22c OFFICE SYMBOL
DAVID A GLASGOW, Major, USAF	(202) 767-4937	AFOSR/NA

Initiation, Growth, and
Coalescence of Small
Fatigue Cracks

Annual Scientific Report of
Research conducted during
period 15 January 1983 to
14 January 1984 under
Air Force Grant No.
AFOSR-82-0041A

DTIC
SELECTED
FEB 1 9 1985
A

prepared by

A.F. Grandt, Jr.
School of Aeronautics and Astronautics
Purdue University
West Lafayette, Indiana 47907

CONTENTS

        B.J. Heath and A.F. Grandt, Jr., "Stress Intensity
        Factor for Coalescing and Single Corner Flaws
        Along a Hole Bore in a Plate"

        R. Perez and A.F. Grandt, Jr., "Coalescence of
        Multiple Fatigue Cracks at Notch"

        A.F. Grandt, Jr., R. Perez, and D.E. Tritsch,
        "Cyclic Growth and Coalescence of Multiple
        Fatigue Cracks"

        A.F. Grandt, Jr., A.F. Thalker, and D.E. Tritsch,
        abstract for paper entitled "An Experiment and
        Numerical Investigation of the Growth and
        Coalesence of Multiple Fatigue Cracks at Notches"

1.0 INTRODUCTION

This Annual Scientific Report summarizes research accomplished during the second year (January 83 to January 84) of AFOSR Grant No. AFOSR-82-0041A. The objective of this effort is to determine the manner in which "small" fatigue cracks initiate at notches, extend by cyclic loading, interact with adjacent flaws, and coalesce into a single dominant crack which controls final fracture. The desired product is a predictive scheme capable of analyzing the early stages of fatigue crack growth which are characterized by the growth and link-up of small cracks. Research toward this goal is directed at the following tasks.

I. Crack Growth Predictive Algorithm. A computer program is being developed to predict the growth and coalescence of multiple cracks located at notches.

II. Crack Interaction Analysis. Stress intensity factors solutions are computed for multiple cracks located at an open hole. These solutions are required for the multiple crack growth algorithm.

III. Crack Coalescence Experiments. Fatigue tests are being conducted with multiply cracked specimens to provide a data base to evaluate the predictive model. Initially the model will be verified with "large crack" results directed toward coalescence aspects of the problem. Subsequent experiments will focus on coalescence of "small" cracks.

IV. Characterization of Small Cracks. This phase of the effort is directed toward the growth and coalescence of physically small cracks. These data will be used to characterize the growth of

"small" flaws, which are expected to behave differently than

"large" cracks.

Additional details of these goals and progress to date are described in
the remaining sections of this report.

2.0 SUMMARY OF PROGRESS AND ACCOMPLISHMENTS

2.1 Task I Progress - Crack Growth Algorithm

A computer program has been written to analyze the multiple crack configurations shown in Fig. 1. Various combinations of surface and/or corner flaws are assumed located along the bore of a circular hole. It is assumed that linear elastic fracture mechanics are valid and that crack growth rates are controlled by the stress intensity factor K. Stress intensity factors are estimated at the major and minor crack axes (locations 1 to 6 in Fig. 1) by modifying the solutions for single cracks in a large body [1] with an interaction factor [2] developed here for coalescing cracks. (The interaction solution is discussed in the Task II progress section). The crack tips are allowed to grow independently at their major and minor axes without specifying crack shape changes. The multi-degree of freedom program predicts the growth of the separate initial cracks and their coalescence into single surface corner, or through-the-thickness flaws as shown in Fig. 2. Sample predictions and comparisons with test data are described in the Task III progress section.

2.2 Task II Progress - Crack Interaction Analysis

A key element of the overall predictive scheme is determining the interaction between adjacent cracks prior to their actual coalescence. The presence of a nearby flaw, for example, causes in increased crack growth rate as the two cracks approach each other. Although a few authors have studied the magnification in stress intensity factors due to coalescing cracks [3-6], solutions were not available for multiple cracks at notches. Thus, one phase of the current effort is

directed toward obtaining stress intensity factor solutions for coalesc-
ing cracks at fastener holes, a geometry which is also studied experi-
mentally in the current program.

The three-dimensional finite element-altering method [7-9] was
used to compute stress intensity factors for symmetric corner cracks
located at opposite sides of a plate containing a hole loaded in remote
tension. Although the analysis was limited to symmetric corner cracks,
several flaw shapes and sizes were considered. By comparing the double
crack results with corresponding solutions for single cracks, it was
possible to determine the effect of the second crack on the stress
intensity factor as the two flaws grow toward each other and eventually
touch.

Additional details of the crack interaction analysis are given in
Refs. 2 and 10. Those results have been described by a crack inter-
action factor which has been incorporated in the computer program
described in Task 1 to account for crack coalescence in the overall
prediction scheme. Experimental verification of the crack coalescence
predictions are described in the following section.

2.3 Task III Progress - Crack Coalescence Experimental Evaluation

This phase of the effort is aimed at evaluating the numerical
scheme described in Task I for predicting the initial growth and
coalescence of multiple cracks located at notches. In order to
separate crack coalescence aspects from "small crack" phenomena, the
initial work involved experiments with coalescence of relatively
"large" cracks. Current work with the small crack problem is described
separately in the Task IV section.

As summarized in References 11 and 12, verification of the predictive crack growth model has included comparison with several sets of experimental data. Both single cracks at holes and multiple coalescing flaws have been studied. The multiple crack configurations include coalescing cracks at open holes in polymethylmethacylate (PMMA) plates (transparent polymer specimens which allow direct observation of the crack plane), PMMA bend specimens, and metal edge notch specimens.

Excellent results [11,12] have been obtained for large corner cracks which coalesce along the bore of an open hole in a PMMA tension specimen (Figure 1c configuration) and for small surface cracks which occur along a semicircular edge notch in metal specimens. The PMMA hole crack data were generated during the present program [13], while the metal data were obtained from another investigation [14].

The metal results described in an earlier progress report [12] were obtained by Dr. A. Thakker with Waspalloy specimens shown in Figure 3. Additional test results have been obtained by Thakker for titanium specimens (Ti-6-2-4-6), and crack growth predictions were performed here. Typical predictions for the titanium small crack coalescence tests are given in Figures 4-7, while Fig. 8 summarizes predicted and test lives for the titanium and Waspalloy experiments. The tests were conducted with the edge notched specimen geometry shown in Figure 3. Crack lengths were measured from fracture surface markings made by heat tinting techniques. (The specimens were periodically heated to oxidize the crack surfaces). Note that the predictive model generally gives an excellent estimate for total specimen life.

2.4 Task IV Progress - Characterization of Small Cracks

It is commonly known that physically small cracks may grow faster than larger flaws subjected to similar stress intensity factor levels. The assumptions regarding continuum behavior and linear elastic material response lose validity as crack lengths become increasingly small. The problem is further complicated by the presence of adjacent flaws which often initiate simultaneously and which interact prior to the coalescence process. The preceeding sections have described tasks directed toward the coalescence problem. This prior work has concentrated on relatively large flaws in order to separate small crack behavior from coalescence phenomena. This section briefly outlines work aimed at the "small crack problem."

A series of fatigue tests have been conducted with V-notched PMMA bend spe. mens. Natural fatigue cracks were allowed to develop along the V-notch and to coalesce into a single flaw. Time lapse photography was used to record and measure the individual and coalescing flaws. Flaw sizes (and shapes) less than 0.005 inches are routinely observed and measured. Typical results are given in References 12 and 13.

In a few tests, the multiple cracks quickly joined to form short through-the-thickness flaws. Stress intensity factors have been estimated for these small cracks, and crack growth rates are compared with baseline data for larger through-cracked specimens in Fig. 9. These preliminary results indicate that small cracks grow faster than large flaws (at similar ΔK levels), as typically observed in structural metals.

Analysis of these tests is complicated by the stress field present at the sharp V-notch. Additional analysis of the notch specimen are

being conducted to verify the small crack behavior shown in Fig. 9, and
to allow predictions for the growth and coalescence of multiple surface
cracks at notches. It is recognized that this goal could be complicated
by nonlinear plastic zone effects which may limit the LEFM approach for
.he small crack tests.

3.0 PLANNED RESEARCH

This section briefly summarizes research planned for the remainder of the proposed effort. For convenience, discussion is organized around the four tasks described in the previous sections.

3.1 Task I Plans - Crack Growth Algorithm

The current crack growth model predicts growth and coalescence of multiple cracks located at circular holes. Linear elastic fracture mechanics are assumed to be valid as stress intensity factors are used to compute crack growth rates.

The multi-degree of freedom predictive program has been written in a modular manner, so that modifications may be made as required. It is expected that new stress intensity factor solutions will be added to analyze alternate specimen geometries (e.g. surface cracked bend and semi-circular notched bend specimens). In addition, should subsequent work indicate that LEFM does not apply to the small crack tests, an alternate crack growth parameter (to ΔK) may be incorporated in the predictive scheme. Current literature on nonlinear crack growth (e.g. Ref. 15) will be studied as appropriate.

3.2 Task II Plans - Crack Interaction Analysis

Currently, the Newman/Raju [1] stress intensity factor solutions for cracked holes, modified with a crack interaction factor [2] to account for multiple cracks, form the basis for the original stress intensity factor solutions. Although these stress intensity factor solutions were derived for cracked holes in large plates, they have been successfully modified with a "correction factor" [11] and applied

to semicircular notches loaded in remote tension (as required for the crack growth predictions shown in Figs. 4-7).

It will be necessary to estimate stress intensity solutions for the other specimen geometries employed in the experimental effort. These other specimen types include the semicircular edge notch, V-notch, and keyhole specimens shown in Fig. 10. In addition, a surface cracked bend specimen is also being investigated. All of these specimens are loaded in four-point bending in a manner which provides direct observation of the crack plane. Although these specimens are readily suited for the experimental work, K solutions are not available for the notched geometries, although Newman and Raju provide results for the surface crack loaded in bending [17]. Stress intensity factors will be estimated for the notched specimens either by the "correction factor" approach successfully employed for the semicircular edge notch tension specimen [11] or by employing the "crack face pressure" stress intensity solutions given in Reference 16. The semicircular notch bend specimen may be examined in more detail with the finite element alternating method employed in Reference 2. The goal here is to obtain reasonable stress intensity factor estimates for the experimental effort, and not to conduct an in-depth stress intensity factor analysis program for various crack configurations.

Currently the interaction factors developed for symmetric corner cracks at holes [2,10] are used to predict the increased growth rates as two cracks approach each other. The present analysis assumes the cracks are symmetric, located at open holes, and lie in the same plane. The results have worked well for cracked holes and semicircular notches loaded in tension. As experimental results are obtained for

nonsymmetric and slightly out-of-plane flaws, it may be necessary to modify the interaction solutions. Again, potential modifications will be "engineering type" estimates, since a rigorous three-dimensional analysis of nonsymmetric, out-of-plane cracks is beyond the scope of the present investigation.

3.3 Task III Plans - Crack Coalescence Experimental Evaluation

The goal here is to further evaluate the multiple crack growth and coalescence scheme through comparison with additional experimental data. To date, successful predictions have been obtained for symmetric coalescing corner cracks at holes in PMMA plates [11,12], and for small surface flaws at semicircular edge notches in Waspalloy [12] and titanium tension specimens (Figs. 3-8). In addition, experimental results [13] have been obtained for coalescing flaws in PMMA bend specimens (both the semicircular and V-notched configurations shown in Fig. 10). As mentioned in Section 3.2, efforts are underway to estimate stress intensity factors for these two notched bend specimens. When completed, those solutions will be incorporated in the life prediction program and predictions made for these PMMA test results.

To expand the evaluation to a larger data base, tests are being conducted with polycarbonate specimens. Polycarbonate is also a transparent polymer, but exhibits considerably more ductility than PMMA. Baseline fatigue crack growth data have been collected for the polycarbonate material and are given in Fig. 11. Note that stable fatigue crack growth rates (da/dN) are obtained at ΔK levels of 3,000 psi-in$^{1/2}$ for the polycarbonate, while as shown in Fig. 9, K_{I_c} for the PMMA is on the order of 1000 psi-in$^{1/2}$. (Specific K_{I_c} measurements will

will be performed for both the PMMA and polycarbonate test material, along with stress/strain curves.

Polycarbonate crack coalescence tests are being conducted with cracked hole tension specimens and with a surface cracked bend geometry. Experiments have also been conducted with the notched bend specimens shown in Fig. 10. The cracked hole tension specimen shown in Fig. 12 has been analyzed by several investigators [1,2,7,16], and K solutions are well established for many flaw shapes. In addition, existing finite element-alternating method computer codes [2,16] may be applied to analyze new flaw shapes of interest to the current effort.

The flawed hole specimen is somewhat awkward for experimental work, however, since grips must be glued to the specimen ends and the crack plane viewed with a mirror. More significant, however, is the fact that relatively large hole sizes are employed. Although this is not a disadvantage for coalescence tests with "large" cracks, where large sta.ter flaws can be employed, the specimen is not as suited to small crack studies. Since the hole radius is farily large, natural flaws would not be expected to initiate in the same plane, and the coalescence study would be complicated by out of plane cracks. (see Figure 13) Although it will eventually be necessary to study the influence of out-of-planeness on crack coalescence, it appears preferable to initially study flaws which grow and coalesce in the same (or nearly same) plane.

In order to employ a notch geometry with a smaller radius of curvature, and, thus, confine crack initiation and growth to the same plane, the V-notch and keyhole specimens shown in Fig. 10 were examined. Both specimens were subjected to four-point bending to

simplify load application and viewing of the crack plane. All of these specimens have worked well for experimental studies on the initiation of small fatigue cracks. Unfortunately, however, the notch tip stresses significantly complicate analysis of the experimental results.

Current work has focused on an unnotched bend specimen. Small starter slots are placed adjacent to each other in the desired location on the tension surface of a beam with a rectangular cross section. The specimen is annealed to remove residual stresses introduced by the preflaws, and the specimens are cycled in four-point bending. Small fatigue cracks develop around the preflaws, and grow, eventually coalescing into a single surface or corner crack. The Newman and Raju stress intensity factor solution for single surface cracks loaded in bending [17] will be modified with the crack interaction factor as before, and incorporated in the life prediction scheme to predict specimen life.

In summary, then, work on this task will concentrate on conducting more crack coalescence tests with polycarbonate and, perhaps, PMMA specimens. Multiply cracked hole specimens will yield data on coalescence of fairly large flaws. It is planned to look at nonsymmetric corner cracks, and surface/corner crack combinations which have not been studied to date. This specimen closely matches the boundary conditions assumed in the current analysis scheme (Task I), and is quite suited for crack coalescence studies. Initiation and coalescence studies with smaller fatigue cracks will employ the bend specimen. Both polycarbonate, and, perhaps, few PMMA tests will be conducted.

As mentioned previously, this specimen yields small, natural cracks, which lie in nearly the same plane.

Although the original proposal suggested a small pilot study with metal specimens, it is not believed that these tests are necessary now, in view of the excellent results which have been obtained with the Waspalloy (Figs. 18 to 23 in Ref. 12) and Titanium (Figs. 4 to 8 in this document) specimens tested by Thakker [14]. It is felt more appropriate to concentrate on further tests with PMMA and polycarbonate specimens, where crack shapes and sizes are more accurately measured, rather than diluting the effort on a small scale program with metal specimens.

3.4 Task IV Plans - Characterization of Small Cracks

The goal here is to characterize the growth of very small fatigue crack sizes to determine if they grow differently than large flaws. Efforts will focus on the growth of single cracks (or widely separated multiple flaws) so that small crack behavior can be separated from coalescence phenomena. Since the cracks must have small physical dimensions, they will be initiated "naturally" at local stress concentrations. It is important that the starter notches have well defined dimensions, so that the local stress level can be determined and appropriate crack parameters computed. Initially, for example, crack growth rates will be correlated with the cyclic stress intensity factor.

Currently the crack photographs are analyzed by projecting the 35 mm negatives onto a screen and measuring the enlarged image (approximately 30 x) to the nearest mm. Since this method is somewhat crude

and cumbersome, a film positioner has been built to measure the film strips under a microscope. The film holder consists of two miciometer positioners mounted perpendicular to each other. The micrometer heads are calibrated in 0.0001 in. increments, allowing x-y coordinates to be located by cross hairs in the microscope and measured quite accurately on the film strip. Steps have been taken to further automate the film reader with electrical readout to display crack lengths automatically in digital form, and, perhaps, be recorded directly for computer analysis. It is felt the new film reader will significantly improve accuracy and reduce the effort required to measure the crack lengths.

In summary, this task will focus on measuring crack growth rates for small flaw sizes in both polycarbonate and PMMA specimens. Stress intensity factors will continue to be used to characterize crack behavior, *unless the results* indicate LEFM is no longer valid. In that case, an alternate crack tip parameter, such as a strain intensity factor or the J integral, may be examined. If necessary, the multicrack growth and coalescence prediction scheme will then be modified to incorporate the new crack growth characterization term.

4.0 PROFESSIONAL PERSONNEL, PUBLICATIONS, AND PRESENTATIONS

4.1 Personnel

A.F. Grandt, Jr. served as principal investigator for the research effort. He was assisted by the following graduate research assistants during the reported phase of the research.

T. McComb Mr. McComb is currently pursuing a M.S. program in the School of Aeronautics and Astronautics. It is expected that a portion of his research will be submitted as a M.S. Thesis.

R. Perez Mr. Perez completed requirements for the Master of Science Degree in Aeronautics and Astronautics in August of 1983 with the Thesis entitled "Cyclic Growth and Coalescence of Multiple Fatigue Cracks Located at Notches." He is currently pursuing a Ph.D. at Purdue under a university fellowship, and continues to conduct research related to the AFOSR grant goals.

J.E. Pope Mr. Pope is currently pursuing a Ph.D. program in Aeronautics and Astronautics.

D.E. Tritsch, a Teaching Assistant supported by other School of Aeronautics and Astronautics Department funds, worked on a Masters Thesis which supports the goals of this research grant. This thesis was completed in August of 1983 and is entitled "Prediction of Fatigue Crack Lives and Shapes."

4.2 Publications and Presentations

The following papers have been published or presented.

B.J. Heath and A.F. Grandt, Jr., "Stress Intensity Factors for Coalescing and Single Corner Flaws Along a Hole Bore in a Plate," Engineering Fracture Mechanics, Vol. 19, No. 4, 1984, pp. 665-673, (copy included in Appendix)

B.J. Heath, Stress Intensity Factors for Coalescing and Single Corner Flaws Along a Hole Bore in a Plate," M.S. Thesis, Purdue University, May 1983.

R. Perez and A.F. Grandt, Jr., "Coalescence of Multiple Fatigue Cracks at a Notch," Proceedings of the American Society of Civil Engineers Engineering Mechanics Division Speciality Conference, Purdue University, May 1983. Paper presented 24 May 1983. (copy included in Appendix)

R. Perez, "Cyclic Growth and Coalescence of Multiple Fatigue Cracks Located at Notches," M.S. Thesis, Purdue University, August 1983.

D.E. Tritsch, "Fatigue Crack Size and Shape Predictions," M.S. Thesis, Purdue University, August 1983.

A.F. Grandt, "Coalescence of Multiple Cracks at Holes," work in progress presentation to ASTM Task Group, Pittsburg, PA, November 1983.

The following reports have been submitted or are in preparation.

A.F. Grandt, Jr., R. Perez, and D.E. Tritsch, "Cyclic Growth and Coalescence of Multiple Fatigue Cracks," accepted for presentation and publication in the Proceedings of the Sixth International Conference on Fracture, New Delhi, India, December 1984. (copy included in Appendix).

A.F. Grandt, Jr., A. Thakker, and D.E. Tritsch, "An Experimental and Numerical Investigation of the Growth and Coalescence of Multiple Fatigue Cracks at Notches," accepted for presentation at the ASTM Seventeenth National Symposium on Fracture Mechanics, Albany, New York, August 1984. Manuscript to be submitted for publication in ASTM STP devoted to conference proceedings. (Extended Abstract included in Appendix).

5.0 REFERENCES AND FIGURES

1. Newman, J.C. and Raju, I.S., "Stress Intensity Factor Equations for Cracks in Three-Dimensional Finite Bodies," NASA Technical Memorandum 83200, Langley Research Center, August 1981.

2. Heath, B.J. and Grandt, A.F., "Stress Intensity Factors for Coalescing and Single Corner Flaws along a Hole Bore in a Plate," Engineering Fracture Mechanics, Vol. 19, No. 4, 1984, pp. 665-673.

3. Kamei, A., and Yokoburi, T., "Two Collinear Asymmetrical Elastic Cracks," Rep. Res. Inst. Strength Materials, Tohoku Univ., Vol. 10, Dec. 1974.

4. Benthem, J.P. and Koiter, W.T., results reported in Compendium of Stress Intensity Factors, by D.P. Rooke and D.J. Cartwright, The Hillingdon Press, 1976, p. 110.

5. Murakami, Y., Nemat-Nasser, S., "Interacting Dissimilar Semi-elliptical Surface Flaws under Tension and Bending," Engineering Fracture Mechanics, Vol. 16, No. 3, pp. 373-386, 1982.

6. Murakami, Y., and Nemat-Nasser, S., "Growth and Stability of Interacting Surface Flaws of Arbitrary Shape," Engineering Fracture Mechanics, Vol. 17, No. 3, pp. 193-210, 1983.

7. Smith, F.W., Kullgren, T.E., "Theoretical and Experimental Analysis of Surface Cracks Emanating from Fastener Holes," AFFDL-TR-76-104, Feb. 1977.

8. Grandt, A.F., Jr., and Kullgren, T.E., "Stress Intensity Factors for Corner Cracked Holes under General Loading Conditions," Journal of Engineering Materials and Technology, Vol. 103, No. 2, April 1981, pp. 171-176.

9. Grandt, A.F., Jr., "Crack Face Pressure Loading of Semielliptical Cracks Located Along the Bore of a Hole," Engineering Fracture Mechanics, Vol. 14, No. 4, 1981, pp. 843-852.

10. Heath, B.J., "Stress Intensity Factors for Coalescing and Single Corner Flaws Along a Hole Bore in a Plate," M.S. Thesis, Purdue University, May 1983.

11. Tritsch, D.E., "Prediction of Fatigue Crack Lives and Shapes," M.S. Thesis, Purdue University, August 1983.

12. Grandt, A.F., Jr., "Initiation, Growth and Coalescence of Small Fatigue Cracks," Annual Scientific Report submitted to AFOSR, May 1983.

13. Perez, R., "Initiation, Growth, and Coalescence of Fatigue Cracks," M.S. Thesis, Purdue University, August 1983.

14. Private correspondence with Dr. A.S. Thakker, Pratt & Whitney Aircraft Corporation.

15. Hartman, G.A., Rajendran, A.M., and Dawicke, D.S., "The Application of a Nonlinear Fracture Mechanics Parameter to Ductile Fatigue Crack Growth," Technical Report AFWAL-TR-83-4023, AFWAL Materials Laboratory, WPAFB, Ohio, December 1982.

16. Grandt, A.F., Jr., and Kullgren, T.E., "Tabulated Stress Intensity Factor Solutions for Flawed Fastener Holes," Engineering Fracture Mechanics, Vol. 18, No. 2, pp. 435-451, 1983.

17. Newman, J.C., and Raju, I.S., "An Empirical Stress-Intensity Factor Equation for the Surface Crack," Engineering Fracture Mechanics, Vol. 15, Nos. 1-2, pp. 185-192, 1981.
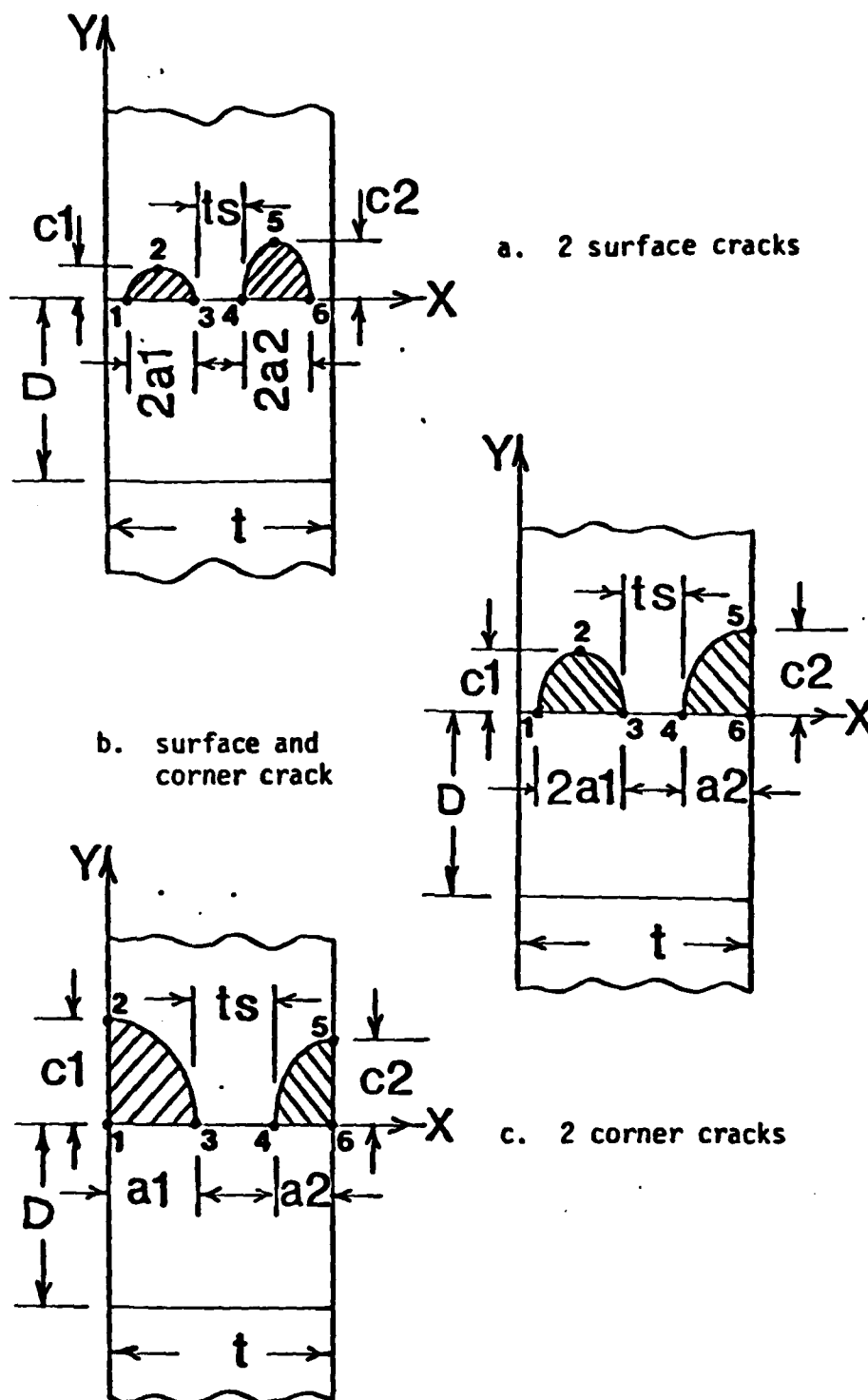
Figure 1   Schematic of multiple cracks located along bore of a hole
in a large plate. Hole diameter is D, plate thickness is t,
and remote tensile stress is applied in z direction.
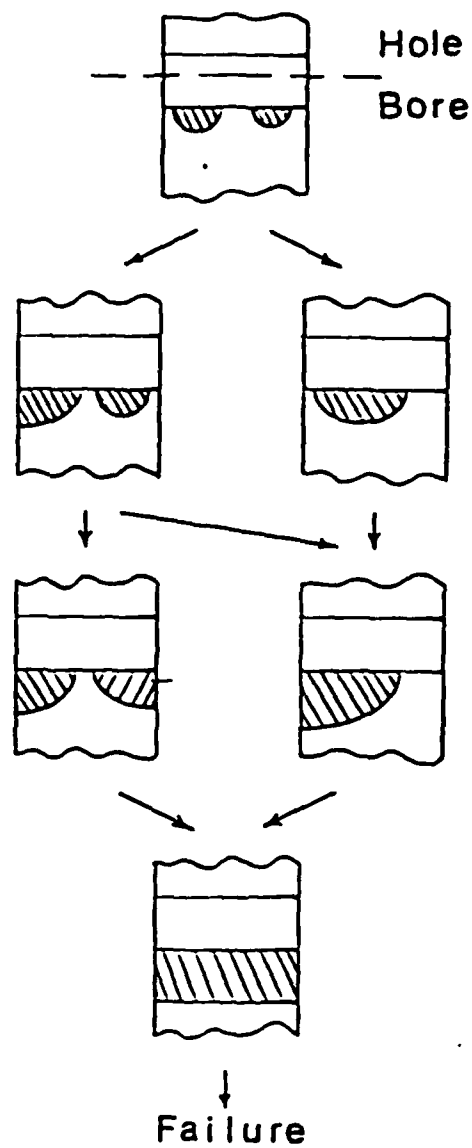
Figure 2   Single and Double Crack Shapes
           Showing Crack Growth Transitions.
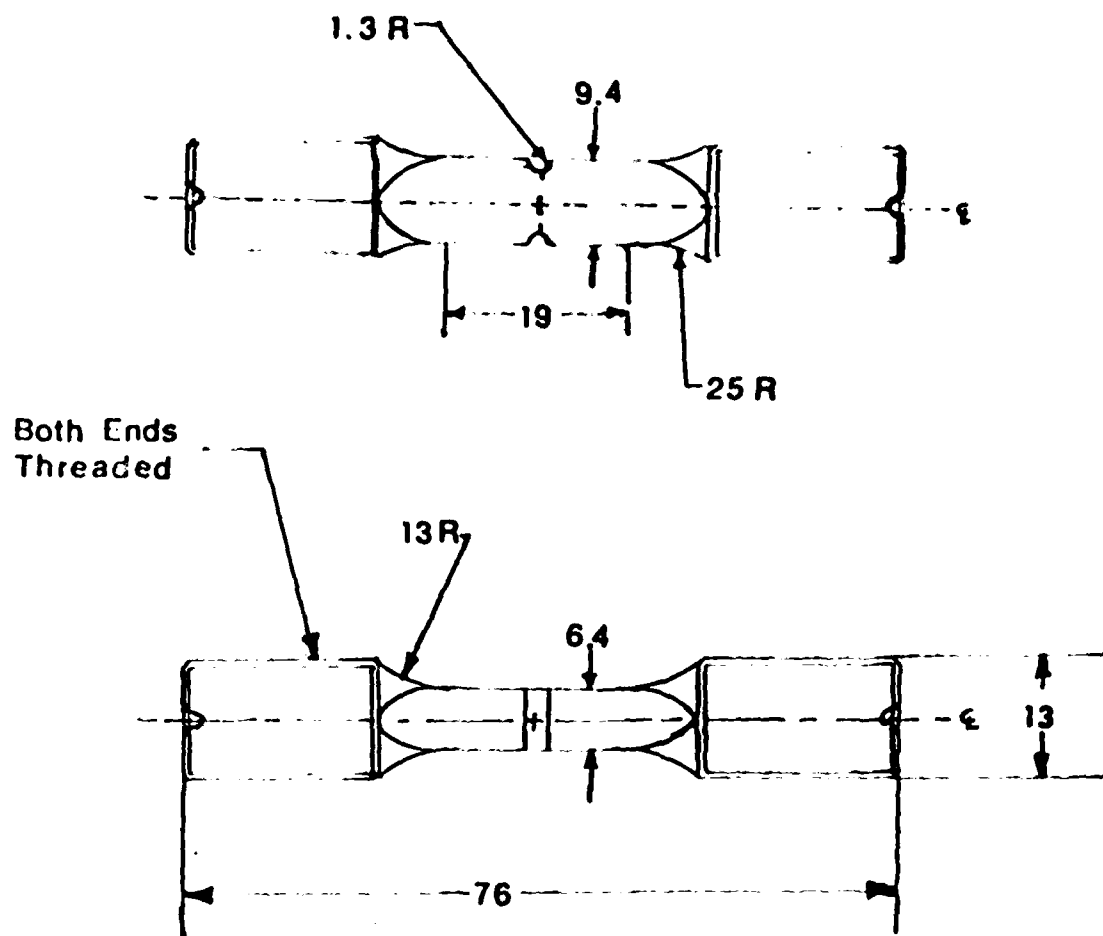
All dimensions are in mm

Figure 3 Drawing of test specimen showing specimen dimensions and location of two semicircular edge notches.

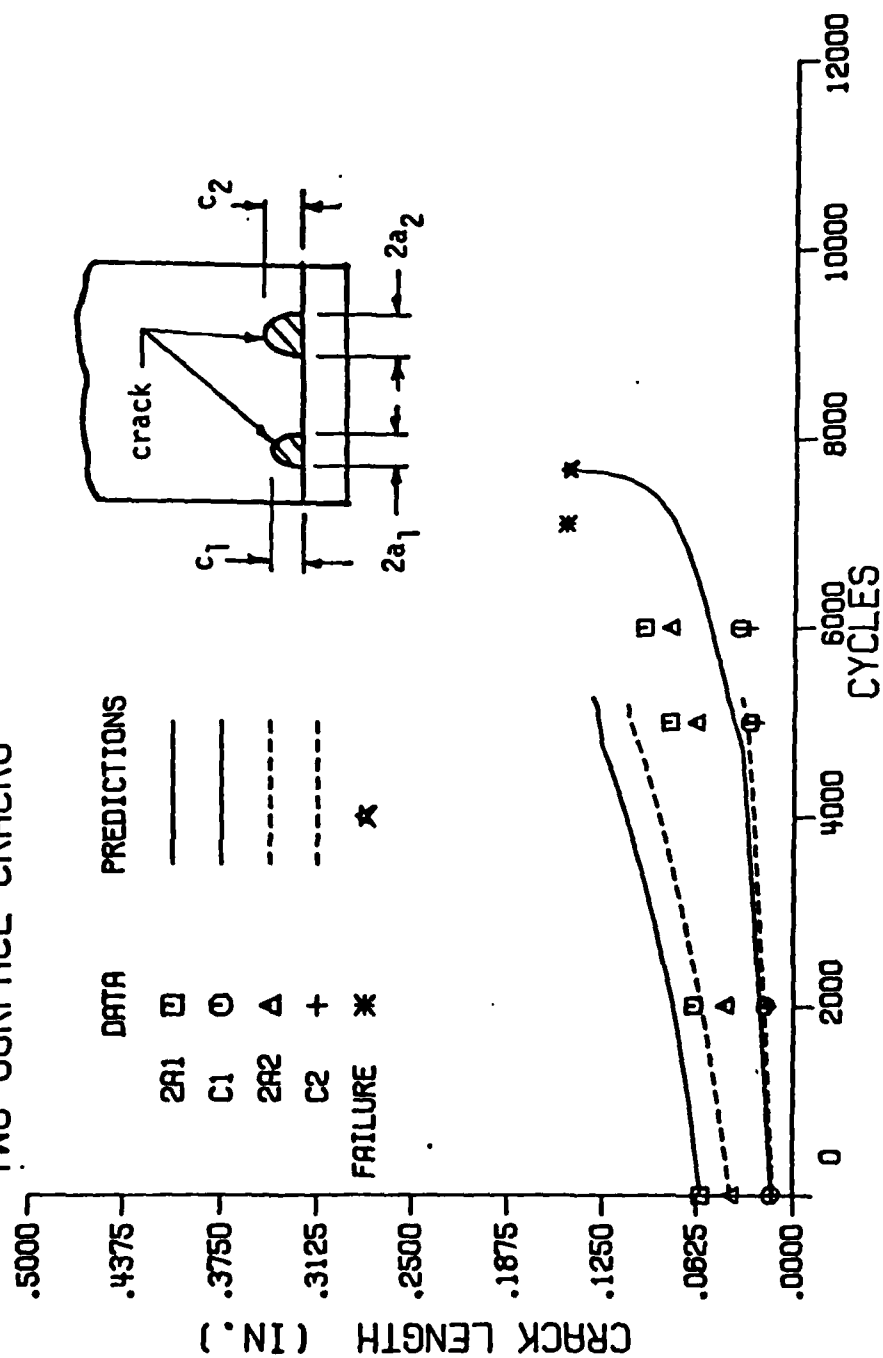Figure 4 Comparison of predicted and experimental growth and coalescence of two surface cracks at semicircular notch in a titanium specimen
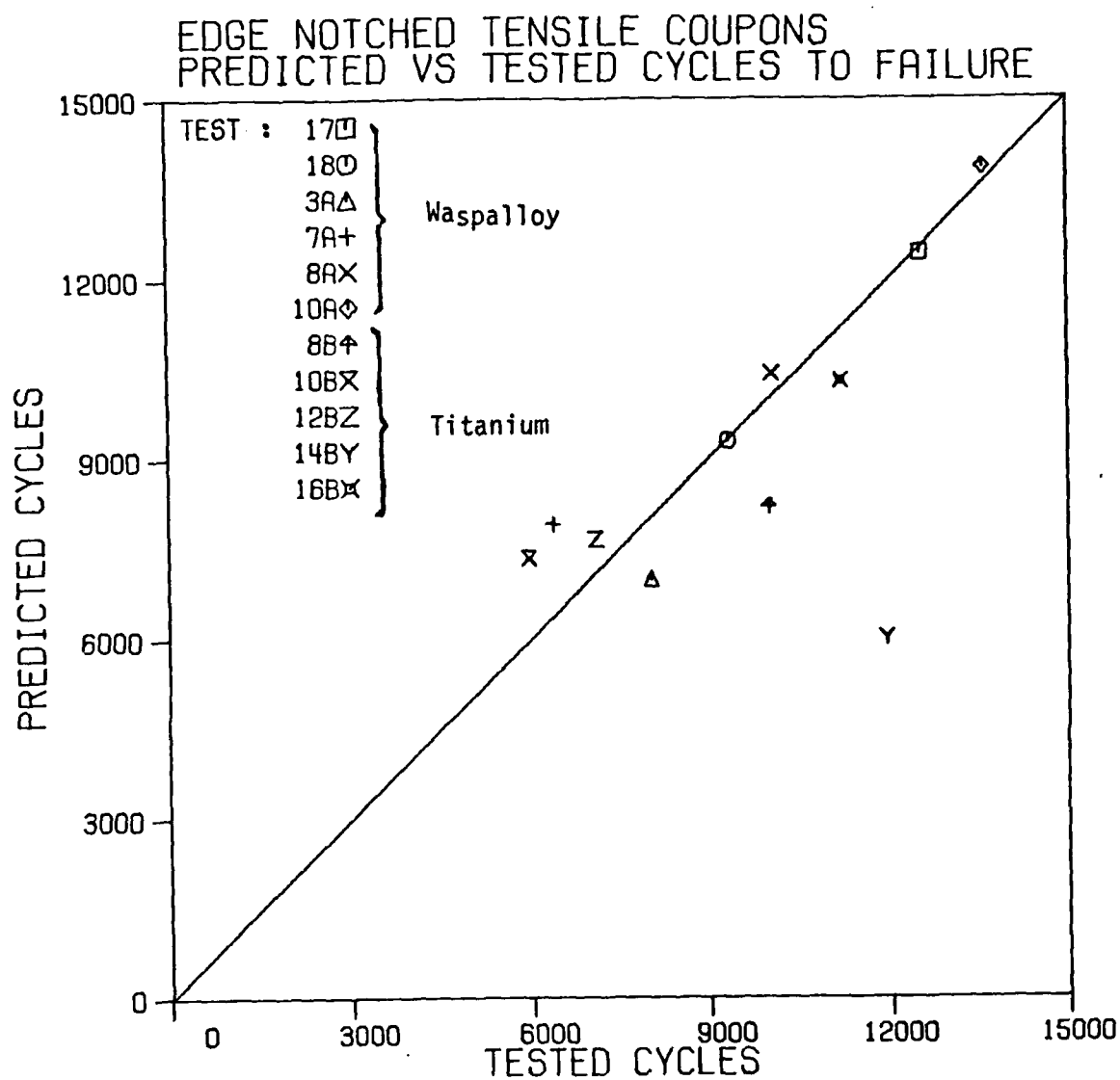
Figure 5   Comparison of predicted and experimental growth and coalescence of two surface cracks at a semicircular notch in a titanium specimen

TEST 12B : EDGE NOTCHED TENSILE COUPON
TWO SURFACE CRACKS

Figure 6   Comparison of predicted and experimental growth and coalescence of
two surface cracks at a semicircular notch in a titanium specimen

Figure 7 Comparison of predicted and experimental growth and coalescence of two surface cracks at a semicircular notch in a titanium specimen

EDGE NOTCHED TENSILE COUPONS
PREDICTED VS TESTED CYCLES TO FAILURE

Figure 8   Comparison of total crack growth life predicted by current
model with results of crack coalescence experiments
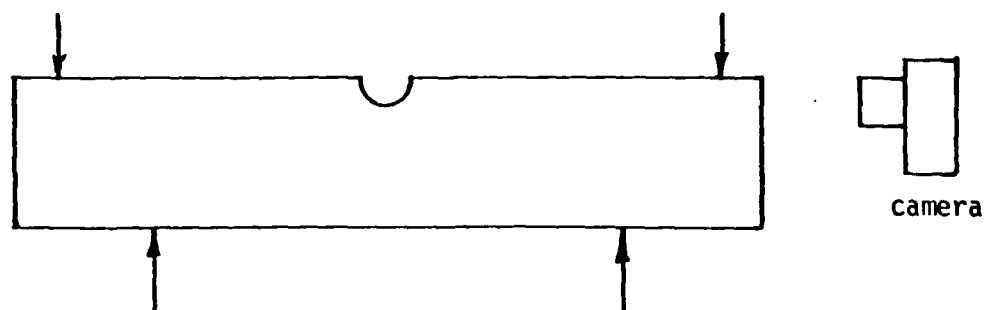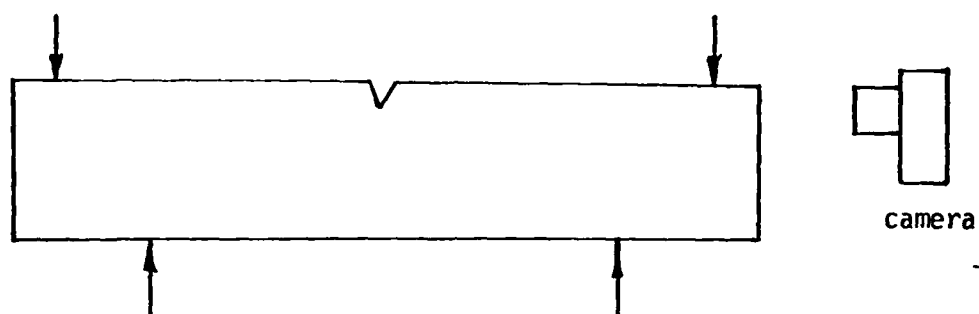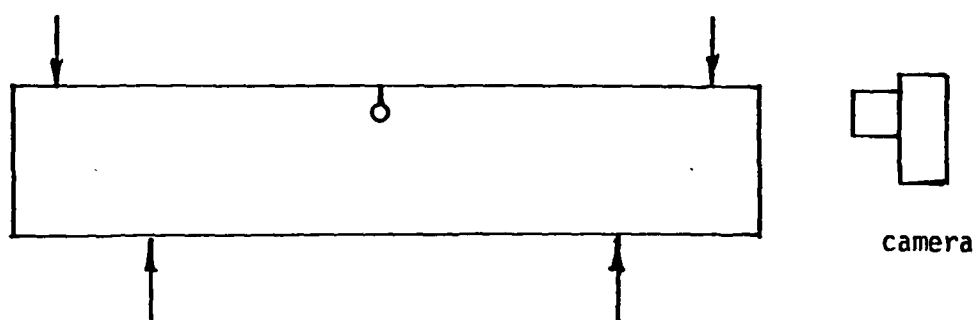conducted by Thakker with Waspalloy and Titanium test specimens.
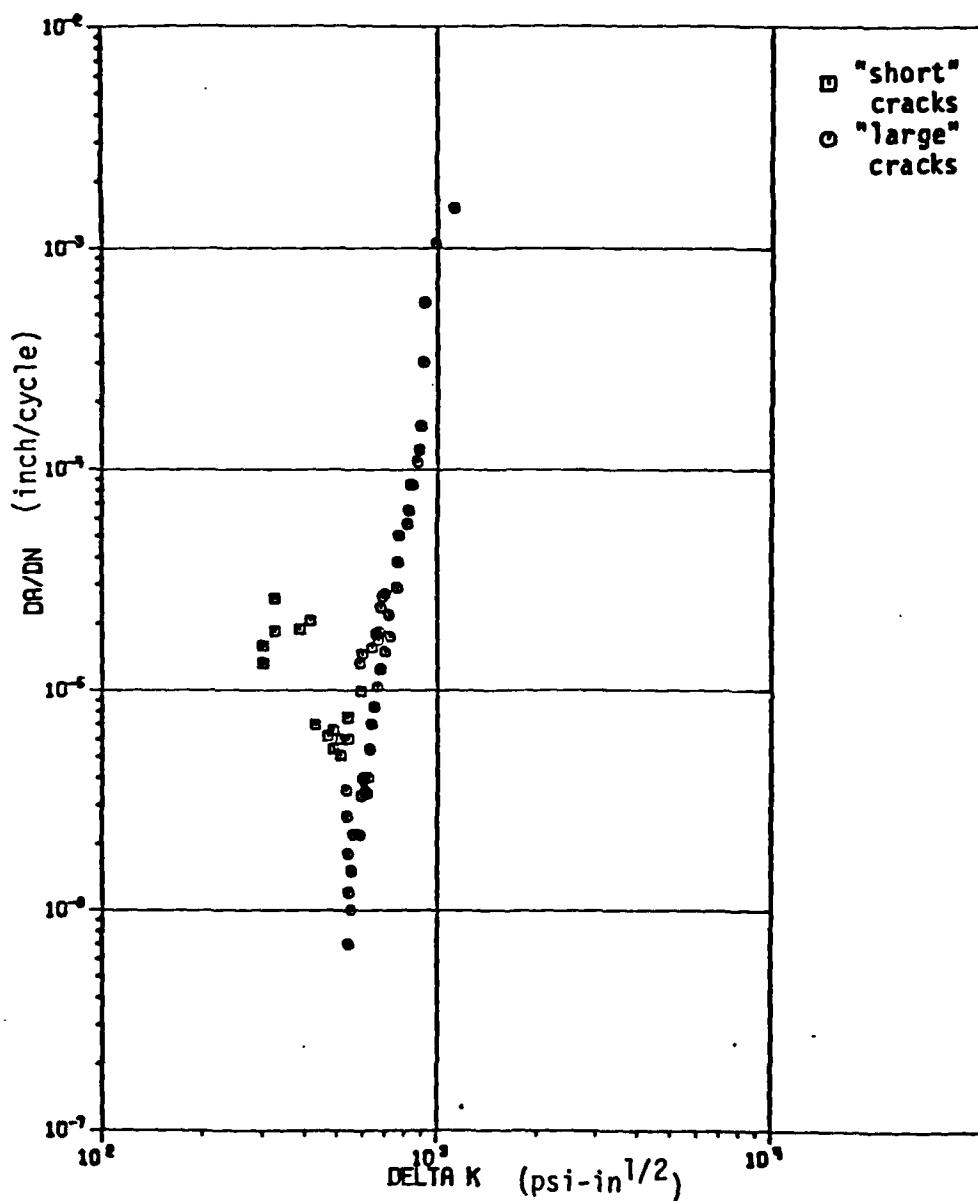
Figure 9 Comparison of "large" and "short" fatigue crack growth
rate da/dN versus cyclic stress intensity factor for
PMMA test material.

semicircular notched bend specimen

V-notched bend specimen

keyhole bend specimen

Figure 10 Schematic drawing of semiciruclar, V-notch, and keyhole specimens showing 4-point bend loading and placement of viewing camera (not to scale).
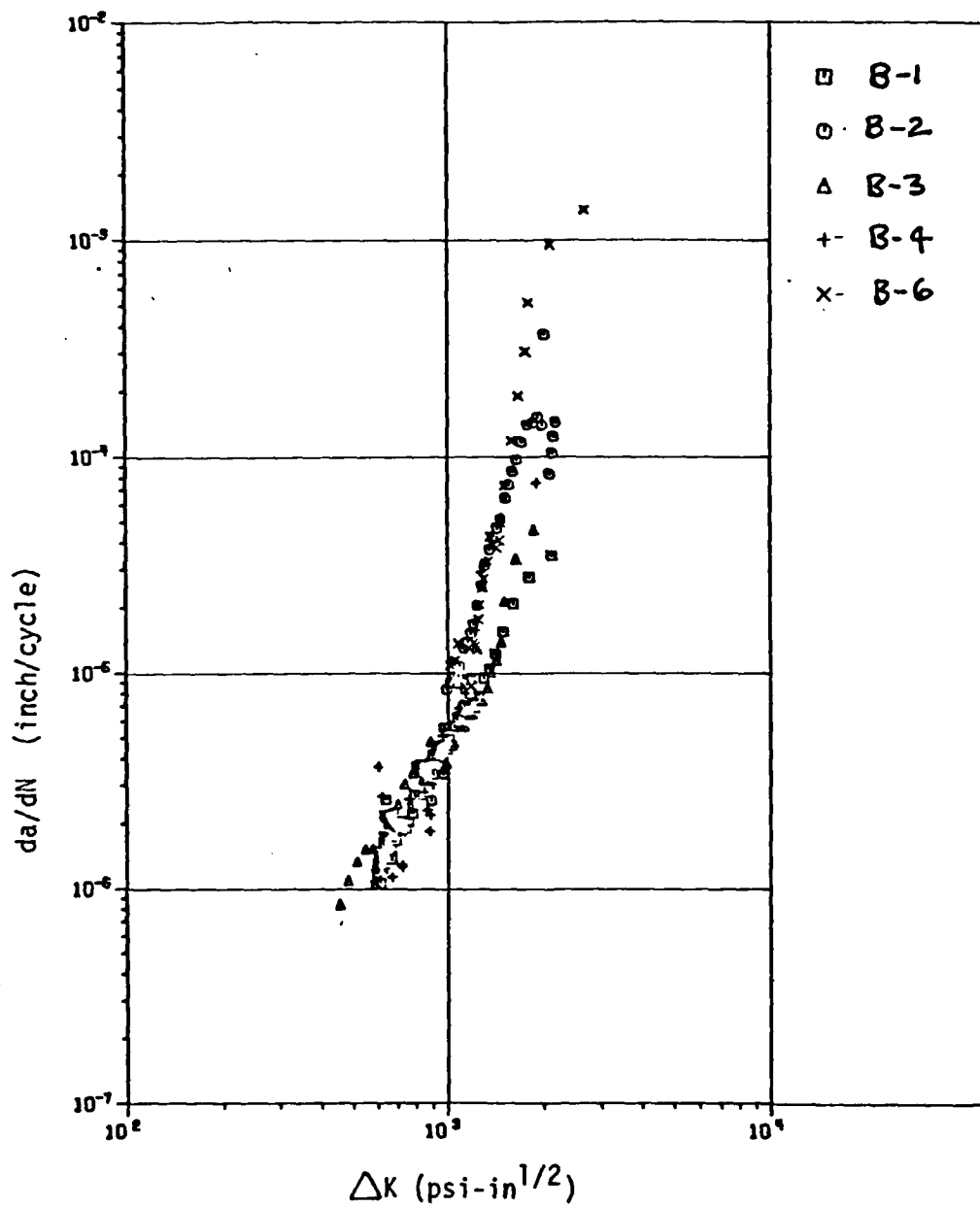
Figure 11   Baseline fatigue crack growth rate da/dN versus $\triangle$K
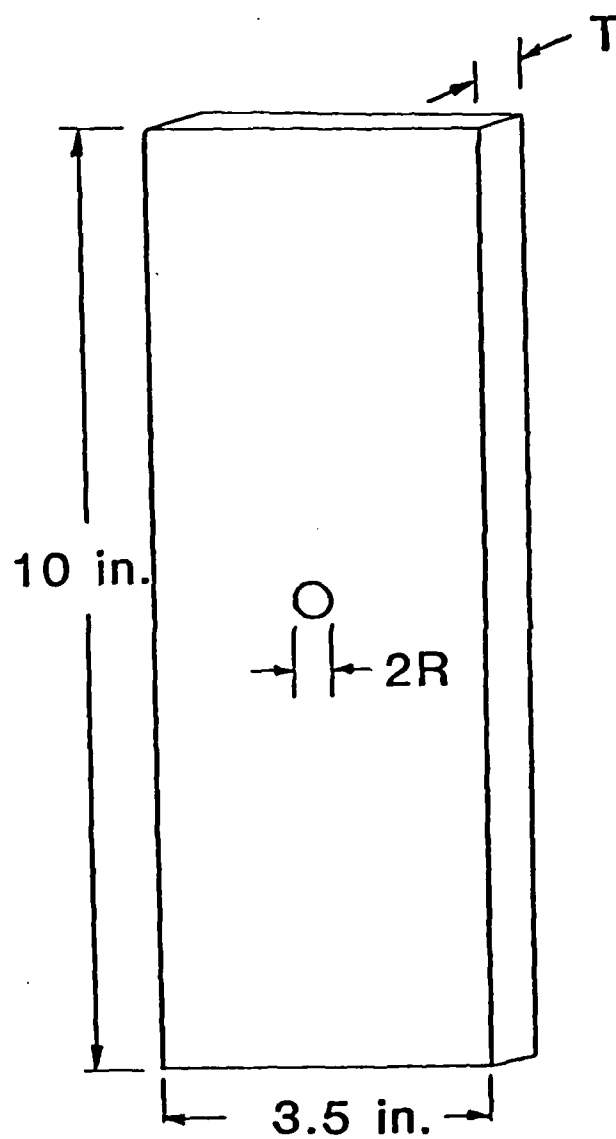for "large" crack polycarbonate test specimens
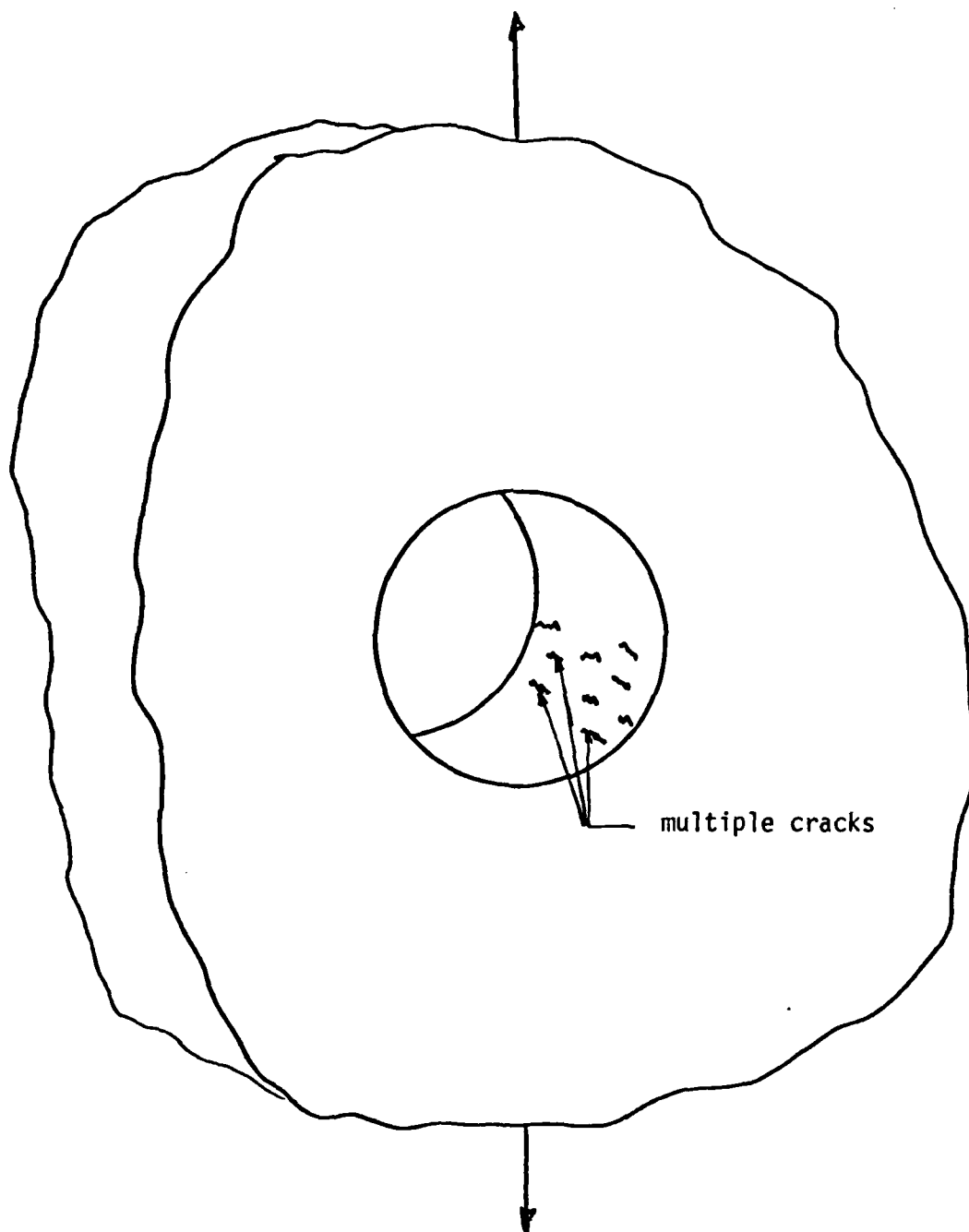
Figure 12 Plate specimen geometry.

Figure 13 Schematic representation of multiple out of plane cracks
forming along the bore of an open hole.

6.0 APPENDIX - Copies of Published or Submitted Papers

B.J. Heath and A.F. Grandt, Jr., "Stress Intensity Factors for Coalescing and Single Corner Flaws," Engineering Fracture Mechanics, Vol. 19, No. 4, 1984, pp. 665-673.

R. Perez and A.F. Grandt, Jr., "Coalescence of Multiple Fatigue Cracks at a Notch," Proc. of the American Society of Civil Engineering Mechanics Division Specialty Conference, Purdue University, May 1984.

A.F. Grandt, R. Perez, and D.E. Tritsch, "Cyclic Growth and Coalescence of Multiple Fatigue Cracks," to be presented and published in Proceedings of the Sixth International Conference on Fracture, New Delhi, India, December 1984.

A.F. Grandt, Jr., A. Thakker, and D.E. Tritsch, Extended Abstract for paper entitled "An Experimental and Numerical Investigation of the Growth and Coalescence of Multiple Fatigue Cracks at Notches." Paper to be presented and manuscript submitted for publication in ASTM STP denoted the proceedings of ASTM 17th National Symposium on Fracture Mechanics, Albany, N.Y., August 1984.

STRESS INTENSITY FACTORS FOR COALESCING
AND SINGLE CORNER FLAWS ALONG
A HOLE BORE IN A PLATE

B. J. HEATH and A. F. GRANDT, Jr.

School of Aeronautics and Astronautics, Purdue University, W. Lafayette, IN 47907, U.S.A.

Abstract—The objective of this paper is to describe the effects of crack interaction on stress intensity factors for two symmetric coplanar corner flaws located along a hole bore. This numerical analysis employes the Finite Element-Alternating Method to determine Mode I stress intensity factors for single and coalescing corner flaws. Using single flaw stress intensity factors as a reference, analysis of crack size and shape effects on K_I for coalescing corner flaws indicates the stress intensity factor for crack points along the hole bore increases as the crack tip separation distance decreases. Interaction effects are not experienced by hole bore crack points when the crack tip separation distance is equal to or greater than half of the largest corner flaw dimension.

INTRODUCTION

NATURALLY occurring fatigue cracks frequently initiate at several independent points along the bore of fastener holes. These individual flaws then grow and coalesce into a single dominant crack which controls final fracture. Prediction of this coalescence phase of crack growth requires stress intensity factor solutions for the individual cracks prior to their "link up" into a single flaw.

It is known that the stress intensity factor for a crack tip is influenced by the close proximity of an adjacent crack tip[1–4]. Crack interaction effects on Mode I stress intensity factors (K_I) have been studied by several authors [1–4]. Various 2-dimensional K_I solutions exist for interaction of coplanar through-the-thickness cracks[3, 4]. Kamei and Yokoburi[3], present a 2-dimensional stress intensity factor solution for two asymmetric through-the-thickness cracks in an infinite sheet, while Benthem and Koiter [4] give a 2-dimensional K_I solution for two symmetric edge cracks. Murakami and Nemat-Nassar [1] present an approximate 3-dimensional K_I solution, obtained by the Body Force Method, for coplanar surface flaws in an unbounded solid. None of these solutions, however, consider coalescence of coplanar flaws located along the bore of a hole in a finite thickness plate. Since multiple fastener hole cracks often occur in service [5, 6], the present paper examines crack coalescence along a hole bore.

The objective of this paper is to describe stress intensity factor results for two adjacent cracks located along the bore of a hole in a finite thickness plate. Figure 1 shows typical plate cross sections for the symmetric and single crack configurations considered. Here a is the crack dimension measured along the hole bore; c is measured along the free surface; T is the plate thickness and D is the hole diameter. The plate is loaded with a remote stress σ applied perpendicular to the crack plane. The Finite

Symmetric Corner Crack
Configuration

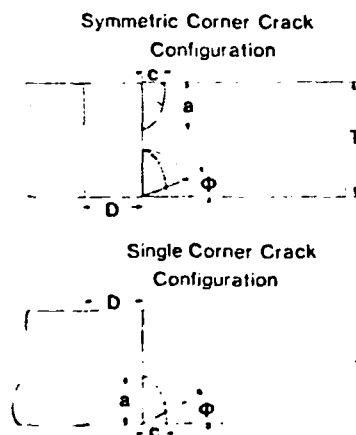Single Corner Crack
Configuration

Fig. 1. Schematic drawing of crack plane showing location of single and symmetric corner cracks located at bore of hole.

Element Alternating Method (FEAM) [7-13] is used to compute K_I for symmetric (coalescing) and single corner cracks along the hole bore.

Results are given in both tabular and graphical form for crack sizes in the range $0.25 \leq a/T < 0.5$ for crack shapes $a/c = 1.11, 1.5, 2.0$ and 3.0. (As described in earlier work [7], numerical programming difficulties prevent analysis of quarter circular cracks, $a/c = 1.0$, with the present computer codes.) Crack shape and size effects on K_I variation around the crack perimeter are presented for coalescing corner flaws. Two and 3-dimensional stress intensity factor solutions for other coalescing crack configurations are compared with the stress intensity factors generated for the corner cracked hole geometry.

NUMERICAL APPROACH

Stress intensity factors for coalescencing cracks along a hole bore are obtained by the Finite Element-Alternating Method (FEAM). The present parametric study makes use of computer codes developed by Smith and Kullgren[7]. The original codes were modified here to treat the coalescing crack problem.

The FEAM calculates K_I based on approximate surface crack boundary conditions. An iterative superposition of two solutions, one a 3-D finite element solution for an uncracked body under prescribed surface loadings, and the second a stress solution for a flat elliptical crack in an infinite body with nonuniform prescribed surface pressure, produce these approximate surface flaw boundary conditions. Earlier applications of the FEAM to various other cracked hole problems are described in Refs [8-12].

The crack coalescence problem studied here requires modification of the finite element mesh and the elliptical crack stress solution of [7] to produce the symmetric crack finite element model used in conjunction with the coalescence option of the FEAM computer code.

Single crack model

The single crack model is a semi-circular plate with a hole. As in Fig. 2, this model has a hole radius R. In order to minimize boundary effects in the region of the crack, the same outer plate radius of $12\,R$ (R = hole radius) used by Smith and Kullgren [7] is used. The single crack model employs 112 20-Node isoparametric finite elements. The hole diameter to thickness ratio (D/T) is 0.5. The modulus of rigidity for the plate is $G = 12 \times 10^6$ psi with a Poisson's ratio of $\nu = 0.3$.

Symmetric crack model

Symmetric interacting cracks were studied by imposing a line of symmetry along the $x = 0.5$ face of the original FEAM model with D/T = 1.0 as shown in Fig. 2. The hole radius, outer radius, and element number are equivalent to the single crack model. In order to account for the line of symmetry, the symmetric crack model has a D/T = 1.0 rather than D/T = 0.5 for the single crack. As shown in Fig. 3, the plane of symmetry imposed along the front surface of the plate, however, effectively doubles the
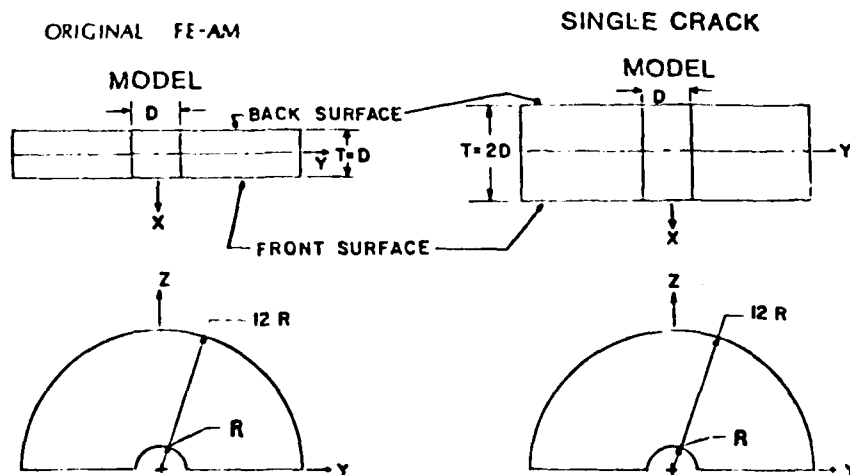

Fig. 2. Geometric models employed for uncracked solution in FEAM iterative algorithm. The half ring geometries shown were modeled by 112 3-dimensional finite elements.
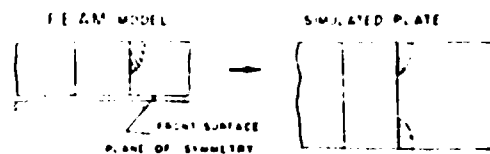
Fig 3 Symmetric crack model showing how front surface plane of symmetry simulates double crack problem.

symmetric crack model plate thickness. Thus, the symmetric crack model D/T equals that of the single crack model (D/T = 0.5). Figure 3 shows how an infinite plate with two symmetric cracks along the hole bore is simulated when a corner flaw is applied to the FEAM symmetric crack model.

DISCUSSION OF RESULTS

Stress intensity factors were generated for crack shapes a/c = 1.11, 1.5, 2.0 and 3.0 by the FEAM analysis. Each crack varied in size from $0.25 \le a/T < 0.5$. The stress intensity factors for the corner flaw configurations considered are listed in Tables 1 and 2. Table 1 lists the stress intensity factor variation for the single crack in 15 degree increments of the elliptic angle ϕ defined in Fig. 1. Stress intensity factor results for the symmetric crack configuration are listed in Table 2.

These results provide a parametric study of size and shape effects on the stress intensity factor variation around the crack perimeter. For a single corner crack with a/c = 1.11, Fig. 4 shows the variation of the dimensionless stress intensity factor $(K_I/\sigma\sqrt{D})$ vs normalized elliptic angle (ϕ/ϕ_{max}) as the crack size (a/T) increases. Note that ϕ_{max} 90 degrees. Figure 5 shows the variation of $K_I/\sigma\sqrt{D}$ over the same a/T range for two symmetric cracks with the same a/c = 1.11.

Recalling that ϕ = 90° corresponds to the hole bore crack location, notice the increased magnitude of

Table 1. Dimensionless stress intensity factors for single corner crack at open hole in a large plate loaded in remote tension. Results given as a function of crack shape a/c, crack size a/T, and position along crack perimeter defined by parametric angle ϕ (ϕ = 0° at front surface and ϕ = 90° at hole bore)

a/c	a/T	$K_I/\sigma\sqrt{D}$						
		ϕ = 0°	15°	30°	45°	60°	75°	ϕ = 90°
1.11	.2500	1.156	1.137	1.137	1.215	1.373	1.553	1.665
	.3000	1.238	1.198	1.183	1.259	1.431	1.633	1.765
	.3500	1.299	1.255	1.234	1.308	1.483	1.692	1.831
	.4000	1.388	1.325	1.285	1.355	1.542	1.773	1.933
	.4500	1.479	1.404	1.347	1.398	1.571	1.794	1.952
	.4750	1.496	1.426	1.371	1.422	1.592	1.813	1.968
	.4875	1.519	1.440	1.378	1.428	1.607	1.840	2.007
	.4938	1.540	1.456	1.388	1.433	1.610	1.844	2.014
1.5	.2500	1.184	1.192	1.202	1.260	1.360	1.457	1.513
	.3000	1.270	1.250	1.237	1.292	1.409	1.535	1.617
	.3500	1.317	1.293	1.279	1.337	1.460	1.591	1.676
	.4000	1.394	1.353	1.326	1.385	1.523	1.676	1.780
	.4500	1.448	1.400	1.362	1.411	1.544	1.695	1.799
	.4750	1.482	1.428	1.383	1.427	1.559	1.712	1.819
	.487.	1.519	1.452	1.395	1.437	1.576	1.741	1.859
	.4938	1.531	1.460	1.399	1.439	1.577	1.743	1.863
2.0	.2500	1.150	1.204	1.247	1.302	1.349	1.357	1.399
	.3000	1.268	1.278	1.284	1.330	1.397	1.437	1.458
	.3500	1.308	1.313	1.315	1.365	1.440	1.490	1.518
	.4000	1.400	1.372	1.351	1.400	1.496	1.573	1.623
	.4500	1.435	1.410	1.386	1.432	1.532	1.596	1.645
	.4750	1.458	1.432	1.407	1.451	1.542	1.615	1.665
	.4875	1.480	1.444	1.414	1.460	1.562	1.646	1.705
	.4938	1.486	1.447	1.413	1.460	1.563	1.651	1.711

Table 1 (Contd)

$K_1/\sigma\sqrt{b}$

a/c	a/T	$\phi = 0°$	15°	30°	45°	60°	75°	90°
3.0	.2500	1.202	1.277	1.311	1.322	1.296	1.182	1.100
	.3000	1.237	1.299	1.335	1.370	1.373	1.256	1.209
	.3500	1.275	1.326	1.358	1.400	1.413	1.339	1.267
	.4000	1.333	1.356	1.373	1.427	1.470	1.423	1.368
	.4500	1.402	1.410	1.411	1.455	1.497	1.454	1.403
	.4750	1.421	1.424	1.421	1.465	1.510	1.470	1.421
	.4875	1.429	1.429	1.428	1.480	1.537	1.505	1.461
	.4938	1.431	1.431	1.430	1.484	1.542	1.511	1.467

Table 2 Dimensionless stress intensity factors for symmetric corner cracks located at intersection of hole bore with front and back surfaces of a plate loaded in remote tension Results given as crack tips approach coalescence (a/T 0.5) in terms of crack shape a/c, crack size a/T, and position along crack perimeter defined by parametric angle ϕ (ϕ 90° at hole bore)

Symmetric Cracks $K_1/\sigma\sqrt{b}$

| a/c	a/T	$\phi = 0°$	15°	30°	45°	60°	75°	$\phi = 90°$
1.11	.2500	1.121	1.145	1.182	1.277	1.422	1.555	1.595
	.3000	1.185	1.201	1.229	1.325	1.479	1.627	1.680
	.3500	1.210	1.224	1.262	1.377	1.560	1.733	1.799
	.4000	1.276	1.283	1.317	1.440	1.643	1.841	1.925
	.4500	1.349	1.347	1.381	1.526	1.765	2.001	2.107
	.4750	1.350	1.356	1.415	1.595	1.872	2.137	2.250
	.4875	1.364	1.356	1.425	1.644	1.981	2.300	2.441
	.4938	1.377	1.347	1.424	1.700	2.127	2.534	2.722
1.5	.2500	1.171	1.219	1.254	1.317	1.398	1.457	1.459
	.3000	1.237	1.273	1.296	1.358	1.450	1.526	1.545
	.3500	1.265	1.301	1.332	1.410	1.523	1.617	1.645
	.4000	1.321	1.352	1.382	1.470	1.601	1.715	1.756
	.4500	1.357	1.385	1.426	1.542	1.709	1.854	1.912
	.4750	1.384	1.409	1.458	1.592	1.784	1.948	2.014
	.4875	1.417	1.425	1.474	1.635	1.872	2.081	2.173
	.4938	1.426	1.406	1.464	1.683	2.010	2.302	2.444
2.0	.2500	1.187	1.261	1.303	1.345	1.373	1.359	1.321
	.3000	1.266	1.326	1.352	1.388	1.422	1.420	1.397
	.3500	1.281	1.345	1.385	1.444	1.501	1.515	1.499
	.4000	1.350	1.394	1.421	1.484	1.562	1.599	1.600
	.4500	1.385	1.432	1.470	1.556	1.661	1.718	1.730
	.4750	1.398	1.446	1.494	1.597	1.719	1.783	1.805
	.4875	1.416	1.452	1.503	1.634	1.797	1.900	1.936
	.4938	1.422	1.433	1.495	1.684	1.932	2.103	2.187
3.0	.2500	1.252	1.357	1.386	1.374	1.313	1.184	1.078
	.3000	1.261	1.372	1.416	1.426	1.386	1.266	1.164
	.3500	1.287	1.387	1.433	1.462	1.450	1.352	1.260
	.4000	1.319	1.418	1.467	1.510	1.516	1.429	1.344
	.4500	1.385	1.458	1.495	1.550	1.585	1.523	1.452
	.4750	1.402	1.472	1.511	1.575	1.622	1.567	1.497
	.4875	1.407	1.471	1.520	1.611	1.690	1.655	1.596
	.4938	1.413	1.460	1.524	1.672	1.823	1.843	1.802
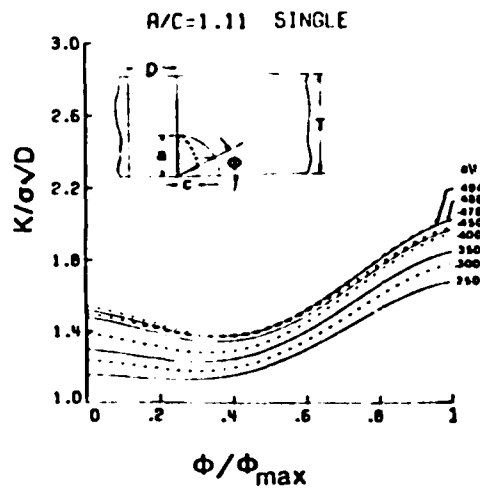
Fig 4. Dimensionless stress intensity factor results for single crack as function of dimensionless parametric angle ϕ/ϕ_{max} ($\phi = \phi_{max} = 90$ at hole bore) and crack size a/T for crack shape $a/c = 1.11$.
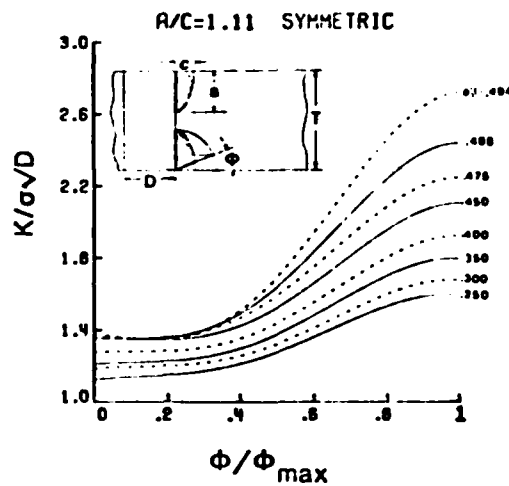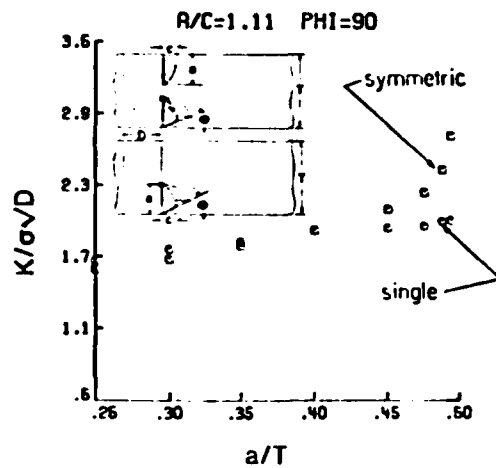

Fig. 5. Dimensionless stress intensity factors for symmetric double crack problem as function of dimensionless parametric angle ϕ/ϕ_{max} ($\phi = \phi_{max} = 90°$ at hole bore) and crack size a/T for flaw shape $a/c = 1.11$.

Fig 6 Comparison of dimensionless stress intensity factors for single and symmetric cracks with aspect ratio $a/c = 1.11$ showing magnification in stress intensity factor at hole bore location ($\phi = 90°$) as crack size a/T increases.

$K_I/\sigma\sqrt{D}$ along the hole bore for the symmetric configuration compared to the same location for the single flaw as the crack size is increased. Using the single flaw $K_I/\sigma\sqrt{D}$ as a reference, the influence of a/T on $K_I/\sigma\sqrt{D}$ for particular flaw points on the symmetric model crack perimeter is shown in Figs. 6-8. For small crack sizes ($0.25 \le a/T \le 0.3$) shown in Figs. 6-8, the single and coalescing configurations differ by a maximum of 4%. However, Figs. 6 and 7 show a significant increase in the symmetric crack $K_I/\sigma\sqrt{D}$ as compared to the single flaw $K_I/\sigma\sqrt{D}$ when the crack size approaches coalescence ($a/T = 0.5$).

Following Murakami [1], a crack interaction factor γ is defined as the ratio of the stress intensity factor for two cracks to the stress intensity factor for a single crack. Kamei and Yokoburi [3] have given 2-dimensional stress intensity factor solutions for two asymmetrical through-the-thickness cracks in an infinite elastic sheet. By equating the crack lengths as shown in Fig. 9(a), and normalizing the crack tip stress intensity factor expression by $\sigma\sqrt{\pi a}$, the interaction factor γ for two symmetric through-the-thickness cracks is obtained. The Benthem and Koiter [4] 2-dimensional stress intensity factor solution for two symmetric edge cracks (see Fig. 9b) may be used to compute the edge crack interaction factor shown in Fig. 10. Here, the double edge-crack solution was divided by the stress intensity factor given by Harris [14] for a single edge-cracked sheet which doesn't bend.
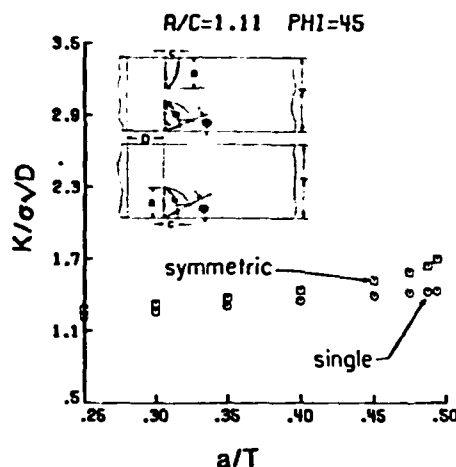

Fig. 7. Comparison of dimensionless stress intensity factors for single and symmetric cracks with aspect ratio $a/c = 1.11$ at crack perimeter location $\phi = 45°$.
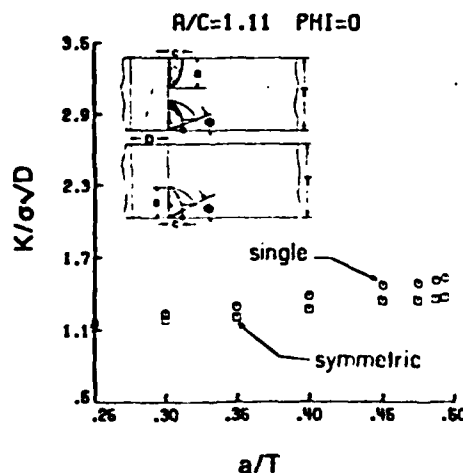

Fig. 8. Comparison of dimensionless stress intensity factors for single and symmetric cracks with aspect ratio $a/c = 1.11$ showing slight decrease in symmetric crack stress intensity factor at surface location ($\phi = 0°$) as crack size a/T increases.
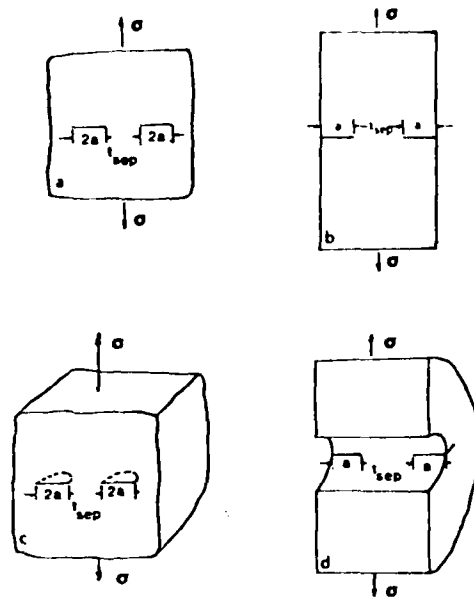
Fig. 9. Interacting crack configurations represented by: (a) Kamei (through-the-thickness center cracks in a large sheet), (b) Koiter and Benthem (through-the-thickness edge cracks), (c) Murakami and Nemet-Nasser (surface cracks in a semi-infinite solid), and (d) present study (symmetric corner cracks located along hole bore).
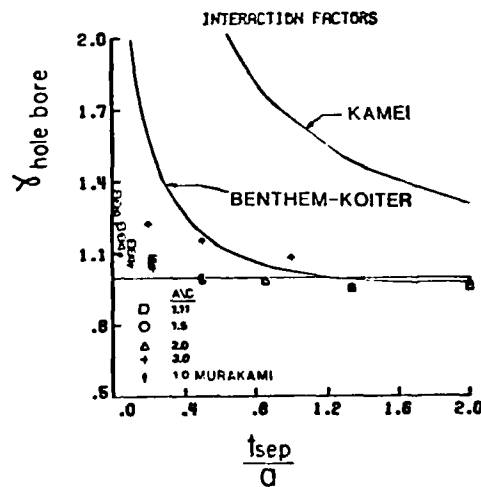

Fig. 10. Comparison of effect of crack spacing t_{sep}/a on stress intensity factor for various 2- and 3-dimensional crack configurations. The interaction factor γ is defined as ratio of double to single crack stress intensity factors.

Three-dimensional crack point interaction factors for symmetric semi-circular surface flaws (Fig. 9c) are presented by Murakami and Nemat–Nassar in Ref. [1]. These coplanar flaws exist in an unbounded solid. The present FEAM results were used to compute 3-dimensional interaction factors for symmetric corner cracks along a hole bore (Fig. 9d). Figure 10 compares these 2- and 3-dimensional crack tip interaction factors as a function of dimensionless crack separation distance (t_{sep}/a). The through-the-thickness interaction factor of Kamei [3] represents the limiting value of two interacting surface cracks, while the Benthem and Koiter [4] edge-crack factor serves as a limiting value for the present study of interacting corner cracks. Due to a numerical instability in the FEAM code, values of crack interaction factors at coalescence $(t_{sep}/a = 0)$ are not obtainable.

Notice the close proximity of the present FEAM results for corner cracked holes to the Murakami [1] interaction factor for surface cracks. As the crack separation t_{sep} exceeds approximately half of the crack length dimension a, $(t_{sep}/a \geq 0.5)$, the FEAM crack interaction factor stabilize at unity, indicating

that the crack tip located along the hole bore is no longer influenced by the adjacent crack. For a given t_{sep}/a, the maximum difference in all hole bore interaction factors presented in Fig. 10 is 10.7%. Figure 10 indicates that crack size (a/T) dominates the increase in K_l due to crack interaction at the hole bore, while crack shape (a/c) has only a slight influence. The effect of crack shape on the hole bore interaction factors is shown on an expanded scale in Fig. 11.

Figure 12 presents the interaction factor at the plate surface $(\phi = 0)$. The factors decrease slightly below unity in the range of $0 < (t_{sep}/a) \leq 0.5$. Figure 12 further indicates that the crack is free of influence from the adjacent crack when the hole bore separation distance is greater than half the crack length a. As the separation distance decreases, the decrease in K_l at the plate surface is considerably less than the increase in K_l at the hole bore location (see Fig. 10). Thus, the effect of crack coalescence is fairly localized, serving to increase K_l for crack points in the vicinity of the hole bore. The free surface K_l, however, is only slightly affected as crack separation approaches zero. Table 3 lists the hole bore and free surface interaction factors for all aspect ratios considered. The decrease in K for the double cracked case may be caused by elimination of through-the-thickness bending for the symmetric crack configuration.

SUMMARY AND CONCLUSIONS

Several conclusions can be made about stress intensity factors for two symmetric coalescing corner cracks. First, as two symmetric corner cracks approach coalescence $(a/T = 0.5)$, the greatest increase in
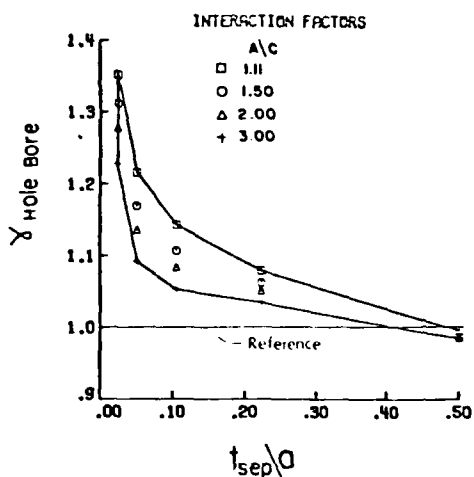

Fig. 11. Summary of the effect of crack spacing t_{sep}/a and crack shape a/c on stress intensity factor interaction at hole bore crack location $(\phi = 90°)$.
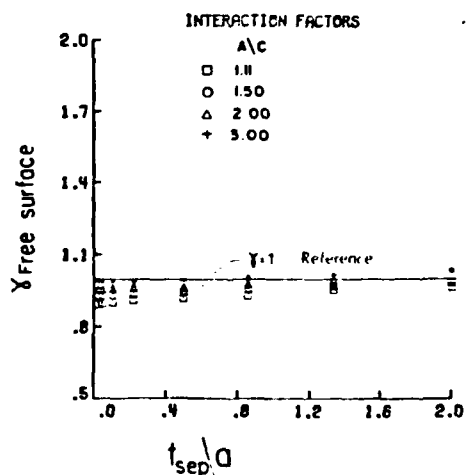

Fig. 12. Summary of the effect of crack spacing t_{sep}/a and crack shape a/c on stress intensity factor interaction at front surface location $(\phi = 0)$ for corner cracked hole.

Table 3. Dimensionless interaction factor, γ, defined as ratio of stress intensity factor for symmetric double crack geometry divided by single corner crack result. Interaction factors given at hole bore ($\phi = 90°$) and free surface ($\phi = 0°$) locations as functions of dimensionless separation along hole bore (t_{sep}/a) and crack shape a/c

		INTERACTION FACTORS γ							
		HOLE BORE ($\phi = 90°$)				FREE SURFACE ($\phi = 0°$)			
	a/c	1.11	1.5	2.0	3.0	1.11	1.5	2.0	3.0
t_{sep}/a	.025	1.352	1.312	1.278	1.228	.894	.931	.957	.988
	.051	1.216	1.169	1.136	1.092	.898	.932	.956	.984
	.105	1.143	1.107	1.084	1.053	.902	.934	.958	.987
	.222	1.079	1.062	1.051	1.035	.912	.937	.965	.987
	.500	.996	.987	.986	.982	.919	.948	.964	.990
	.857	.983	.982	.987	.995	.932	.961	.979	1.009
	1.333	.952	.955	.958	.963	.957	.974	.999	1.020
	2.000	.958	.964	.979	.980	.969	.989	1.033	1.041

stress intensity factor occurs at the crack point along the hole bore. The crack point at the free surface does not experience a significant stress intensity factor increase, but shows a slight decrease in K_I as the crack tips approach along the hole bore.

For crack points along the hole bore, crack interaction (stress intensity factor increase) does not occur until the crack separation distance is equal to or less than half of the crack length a. The localized effect of coalescence is found to depend strongly on crack size (a/T) and only weakly on crack shape (a/c). The crack shape dependence indicates that the deeper cracks (smaller a/c ratios) have a slightly larger K (maximum 10.7% difference) at the hole bore location than more shallow flaws (larger a/c) with the same crack length a.

REFERENCES

[1] Y. Murakami, and S. NemaT-Nasser, Interacting dissimilar semi-elliptical surface flaws under tension and bending Engng Fracture Mech. 16 373–386 (1982).
[2] R. Chang, On crack-crack interaction and coalescence in fatigue Engng Fracture Mech. 16 683–693 (1982).
[3] A. Kamei and T. Yokoburi, Two collinear asymmetrical elastic cracks. Rep. Res. Inst. Strength Materials, Tohoku University Vol. 10 (Dec. 1974).
[4] J. P. Benthem and W. T. Koiter, Results reported in Compendium of Stress Intensity Factors (Edited by D. P. Rooke and D. J. Cartwright), p. 110. The Hillingdon Press (1976).
[5] J. M. Hyzak, W. H. Reimann, and J. E. Allison, The development of quantitative NDE for retirement-for-cause. AFML-TR-78-198, Feb. 1977.
[6] J. H. Harris Jr. D. L. Sims and C. G. Annis, Concept definition: retirement for cause of F100 rotor components. AFWAL-TR-80-4118, Sept. 1980.
[7] F. W. Smith and T. E. Kullgren, Theoretical and Experimental Analysis of Surface Cracks Emanating from Fastener Holes. AFFDL-TR-76-104, Feb. 1977.
[8] T. E. Kullgren, F. W. Smith and G. P. Ganong, Quarter-elliptical cracks emanating from holes in plates. J. Engng Matls and Techn. 100. 144-149 (1978).
[9] T. E. Kullgren and F. W. Smith, The finite element-alternating method applied to benchmark No. 2. Int. J. Fracture 14, R319-R322 (1978).
[10] T. E. Kullgren and F. W. Smith, Part-elliptical cracks emanating from open and loaded holes in plates. J. Engng Matls nad Techn. 101. 12-17 (Jan. 1979).
[11] A. F. Grandt Jr. and T. E. Kullgren, Stress intensity factors for corner cracked holes under general loading conditions. J. Engng Matls Techn. 103(2) 171-176 (April 1981).
[12] A. F. Grandt Jr., Crack face pressure loading of semielliptical cracks located along the bore of a hole. Engng Fracture Mech. 14(4). 843-852 (1981).
[13] F. W. Smith, Stress near a semi-circular edge crack. Ph.D. thesis, University of Washington (1966).
[14] J. O. Harris, Results reported in Compendium of Stress Intensity Factors (Edited by D. P. Rooke and D. J. Cartwright), p. 84. The Hillingdon Press (1976).

Coalescence of Multiple Fatigue Cracks at a Notch

R. Perez* and A.F. Grandt, Jr.**

This paper describes experimental results from fatigue tests conducted with semicircular notched polymer specimens which contained two cracks as shown schematically in Fig. 1. The two corner cracks were located at opposite sides of the semicircular notch, with the left crack defined by the lengths a_1 and c_1, and the right crack by dimensions a_r and c_r as shown in Fig.1b. In the same figure, d represents the crack separation.

a. Four-Point Bend Specimen

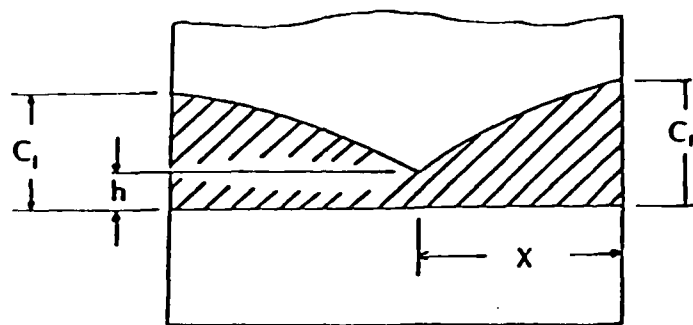b. Corner crack dimensions before coalescence
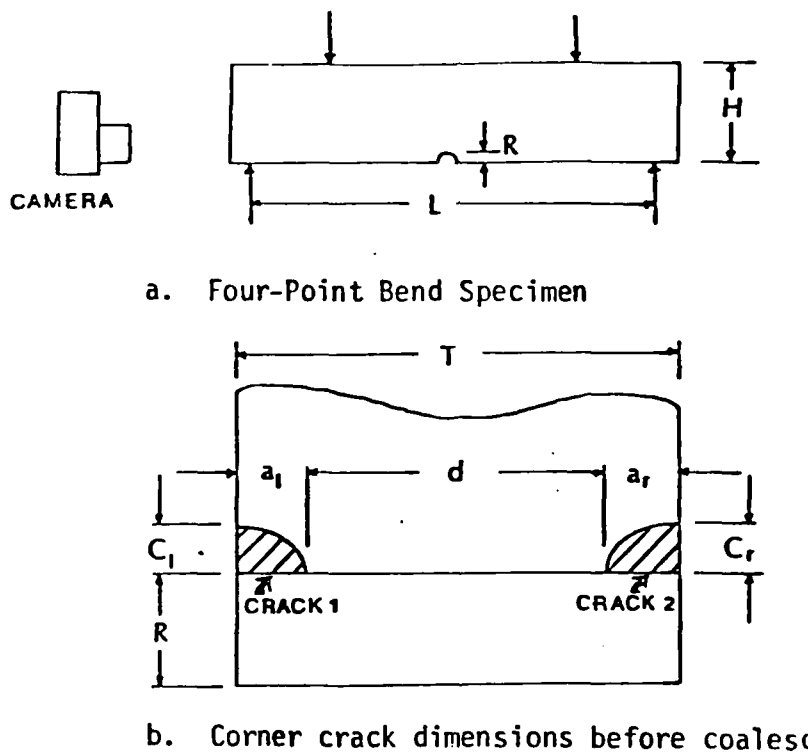
Fig. 1 Specimen geometry showing location of the camera and schematic views of the crack plane.

Five experiments were completed and represented cases of symmetric, nonsymmetric, in plane and out of plane cracks. In each test, the pre-cracked specimen was subjected to cyclic bending and subsequent crack growth photographed through the ends of the transparent specimen. As the fatigue cracks grew the spacing d decreased to zero and the two separate cracks coalesced into a single flaw with the cusped shape shown in Fig. 1c. Projected images of the crack photographs were

*Research Assistant and **Associate Professor, School of Aeronautics
and Astronautics, Purdue University, W. Lafayette, Indiana 47907

1

enlarged, measured, and scaled to actual size and the data recorded in graphical form. Figs. 2 and 3 illustrate two representative graphs.

c. Crack dimensions after coalescence

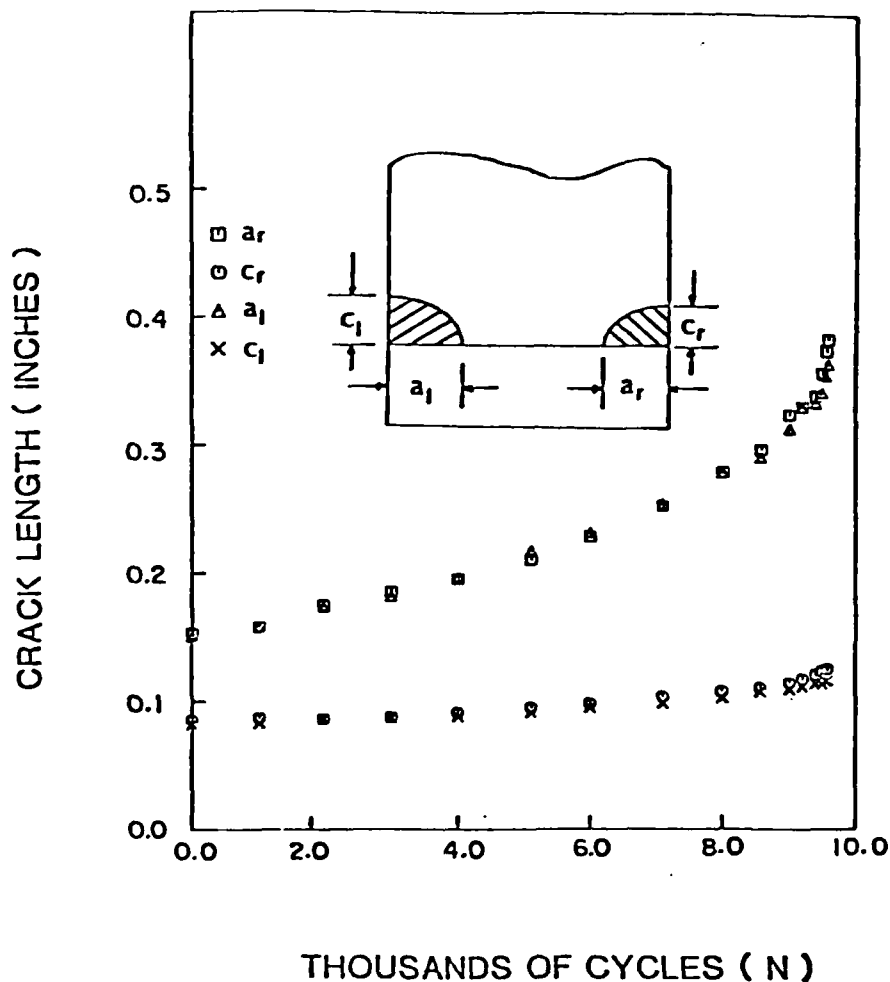Fig. 1(Cont.) Specimen geometry showing location of the camera and schematic views of the crack plane.

THOUSANDS OF CYCLES (N)

Fig. 2 Crack growth before coalescence as a function of elapsed cycles for symmetric out of plane crack test T-5.

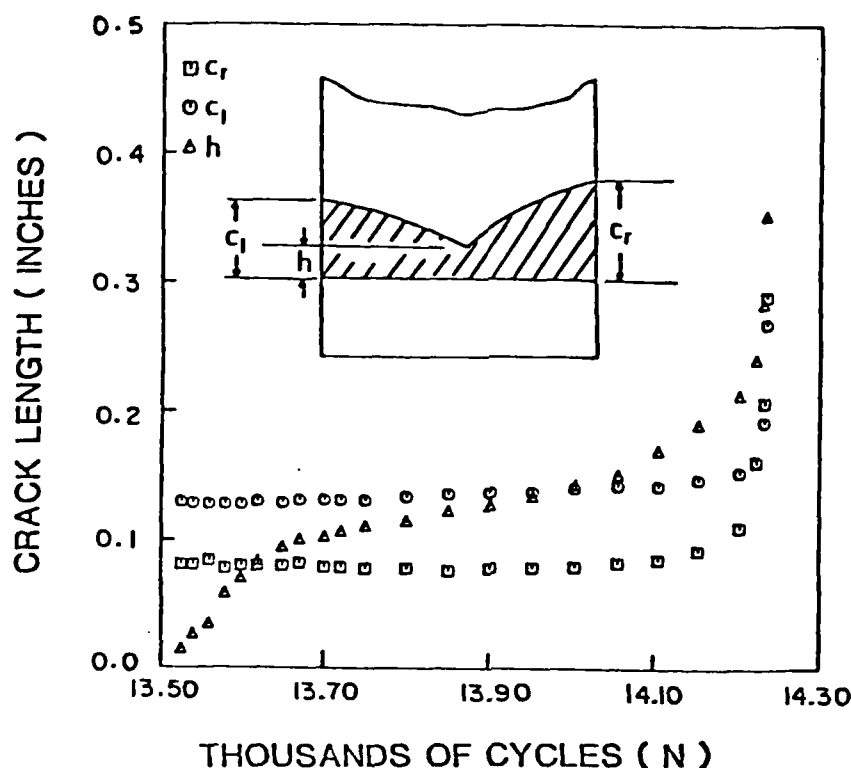2   Perez and Grandt

Fig. 3 Crack growth after encounter and coalescence as a function
of elapsed cycles for nonsymmetric out-of-plane crack
test T-4.

It was observed that interaction effects between cracks were more
pronounced at the crack bore dimension (a) than at the crack surface
dimension (c). Interaction was characterized by an increased rate of
growth of the bore crack length as shown in Fig. 4. This figure was
obtained by shifting the crack growth curve for the small crack horizon-
tally until both cracks had equal initial sizes. In a study of stress
intensity factors for interacting surface cracks Murakami and Nemat-
Nasser [1] point out that if the distance between the centers of two
semielliptical cracks is greater than the addition of the length of the
smaller crack and half the length of the larger, then the cracks will
not influence each other. Although this criterion for crack interac-
tion involves surface flaws in plates, it was applied successfully in
this study of interacting corner cracks along a notch.

Out of plane cracks grew past each other without linkup, and flaw
growth along the notch stopped. Crack growth perpendicular to the
notch and into the specimen interior continued so that a flat crack
front formed in this direction. The crack tips at the hole bore even-
tually curved into each other and coalescence occurred. In plane
cracks simply coalesced to form a through-the-thickness crack.

After the cracks grew past each other in the out of plane crack
tests, the cusp dimension h grew very fast initially, but later slowed
down when a uniform flaw developed. Similar, but less pronounced, cusp
behavior was observed in the in plane crack test.

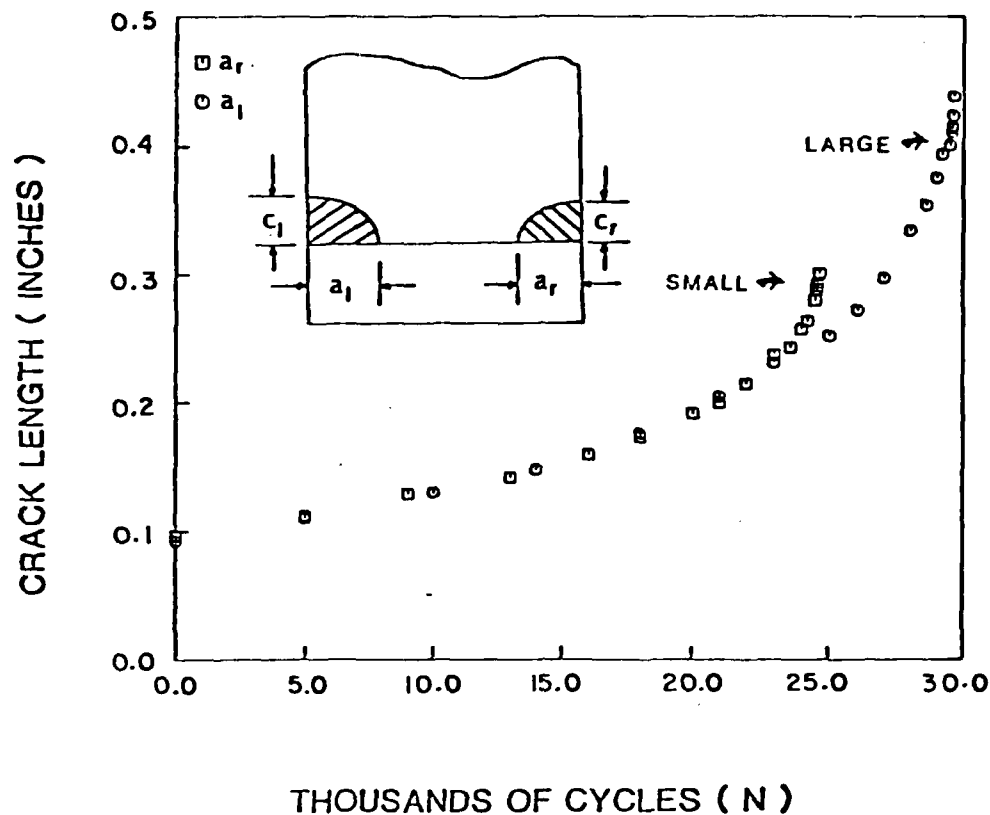3   Perez and Grandt

Fig. 4   Comparison between the crack growth curves of the small and large cracks of test T-2.

Reference

1.   Murakami, Y. and Nemat-Nasser, S., "Interacting Dissimilar Elliptical Surface Flaws Under Tension and Bending," _Engineering Fracture Mechanics_, Vol. 16, No. 3, pp. 373-386, 1982.

4   Perez and Grandt

CYCLIC GROWTH AND COALESCENCE OF
MULTIPLE FATIGUE CRACKS

A.F. Grandt, Jr.*, R. Perez** and D.E. Tritsch**

*Professor and **Graduate Assistant,
School of Aeronautics and Astronautics,
Purdue University
West Lafayette, Indiana 47907 U.S.A.

ABSTRACT

This paper describes an analysis scheme for predicting the fatigue life of
components which contain multiple cracks. Fracture mechanics techniques
are used to predict the initial growth and coalescence of two or more cracks
located along the bore of a hole. The results of experiments with multiply
cracked specimens are described and are compared with crack growth predic-
tions obtained by the analysis method.

KEYWORDS

Fatigue cracks, crack coalescence, fatigue life predictions

INTRODUCTION

Fatigue cracks frequently initiate simultaneously near stress concentrations
formed by notches. These cracks may grow independently for a period, and
then, depending on their initial spacing, may join into a single dominant
crack which causes eventual failure. The objective of this paper is to
describe an experimental and numerical program directed at predicting the
growth and coalescence of multiple fatigue cracks located at holes in
plates.

The particular geometries of interest are shown in Fig. 1. Here 2r is the
diameter of an open hole in a plate of thickness 2t. Initial surface and
corner flaws, which are described by portions of ellipses with semi-axis
dimensions a and c, are located along the bore of the hole. In the present
work, the two separate cracks are assumed to be coplanar, and a remote
tensile stress is applied perpendicular to the crack plane. Various combi-
nations of surface and corner cracks are considered. The next section
presents a life prediction scheme for calculating the time required for the
initial flaws to grow together, coalesce into a single crack, and extend
to final failure. The following section then describes experiments with
multiply cracked specimens conducted to evaluate the numerical analysis.
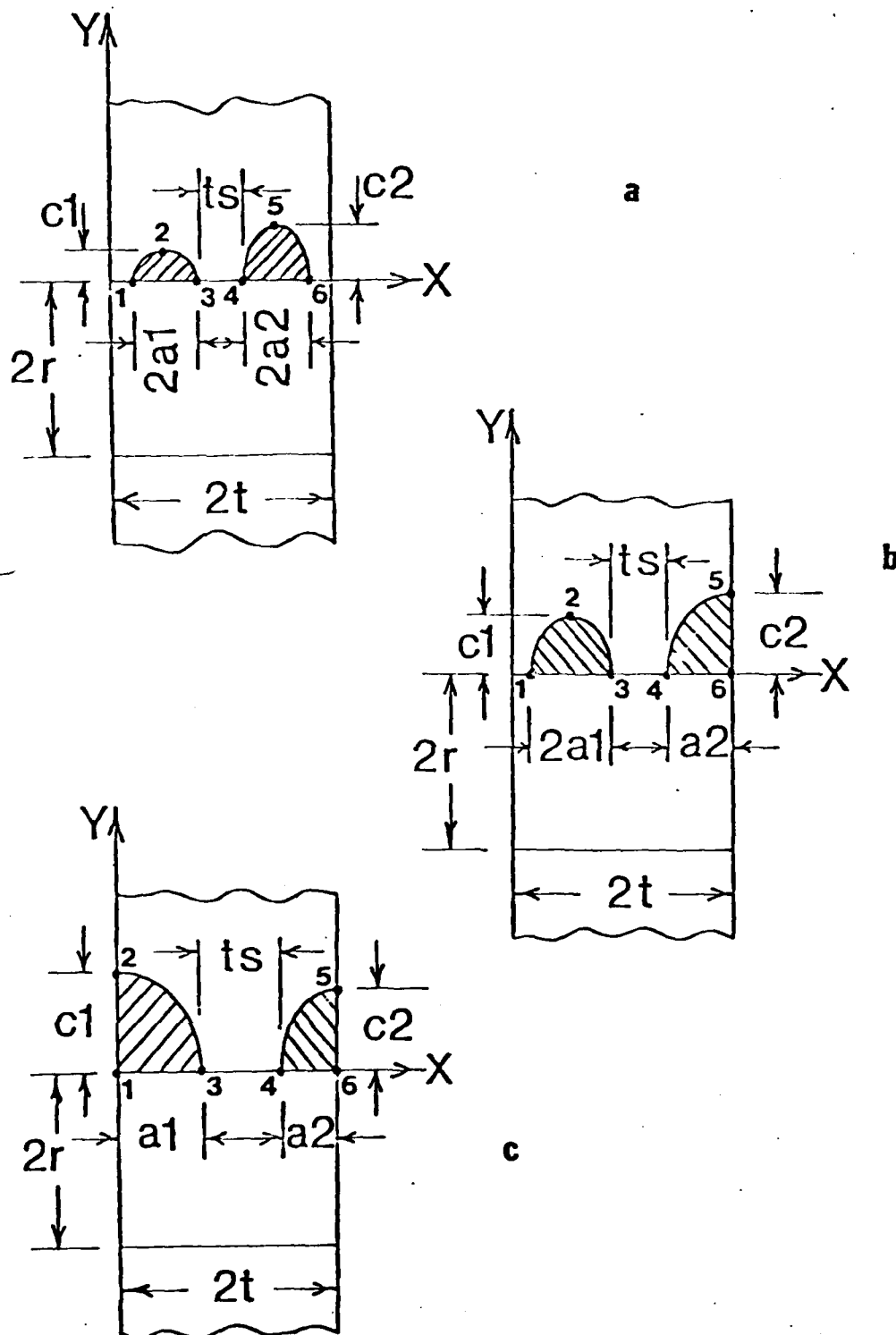
Fig. 1. Two cracks at the bore of a hole defining
crack lengths and crack tip locations.

NUMERICAL ANALYSIS

The goal here is to describe an approach for predicting the initial growth
and eventual coalescence of separate cracks located along the bore of a hole.
The geometries of interest are summarized in Fig. 1. The semi-axis dimension
along the hole bore is given by a, while the crack depth is specified by c.
Subscripts 1 and 2 refer to cracks 1 and 2 respectively. Crack tip locations
are defined by points 1 thru 6 as shown in Fig. 1.

When subjected to an applied stress, cracks 1 and 2 will grow. Let the fati-
gue crack growth rates for crack tips 1, 2, ..., 6 be d1/dN, d2/dN, ...,
d6/dN. Note that, in general, these crack growth rates will have different
values. The crack growth increments for a specified number of cycles ΔN of
loading are, however, related. Assume, for example, that the depth c_2 of
crack 2 extends a small amount $\Delta 5$ during the interval ΔN. Now, ΔN is given
by Eq. 1.

$$\Delta N = \frac{\Delta 5}{\frac{d5}{dN}} \tag{1}$$

The growth Δi of crack tip i is given by

$$\Delta i = \frac{di}{dN} \cdot \Delta N = \frac{di}{dN} \cdot \frac{\Delta 5}{\frac{d5}{dN}} \tag{2}$$

where i takes the values 1 to 6 as appropriate.

Now, if the cyclic stress intensity factors ΔKi are known at crack tips 1,
2, ..., 6, the conventional fracture mechanics approach may be used to
compute the corresponding fatigue crack growth rates (at the various crack
positions) from Eq. 3.

$$\frac{di}{dN} = F(\Delta Ki) \tag{3}$$

Here di/dN is the crack growth rate at location i and F (ΔKi) is the appro-
priate fatigue crack growth model for the material of interest.

Stress intensity factors for the multi-cracked holes were obtained in the
following manner. First, the Newman and Raju (1981) solutions for single
surface or corner cracks located at holes were used to compute K at crack
tip locations 1 thru 6. Newman and Raju (1981) have fit empirical equations
to earlier finite element results obtained for the single crack geometries.
Their empirical solutions are readily coded for computer use, and provide
an effective means for interpolating between the original finite element
results obtained for discrete crack shapes.

The effect of the adjacent flaw was accounted for by an "interaction factor"
obtained previously by Heath and Grandt (1984). In that work, the
three-dimensional finite element- alternating method was used to compute
stress intensity factors for symmetric corner cracks located on opposite
sides the plate thickness (the symmetric version of Fig. 1c). The double
crack K was then divided by the corresponding result for a single flaw to
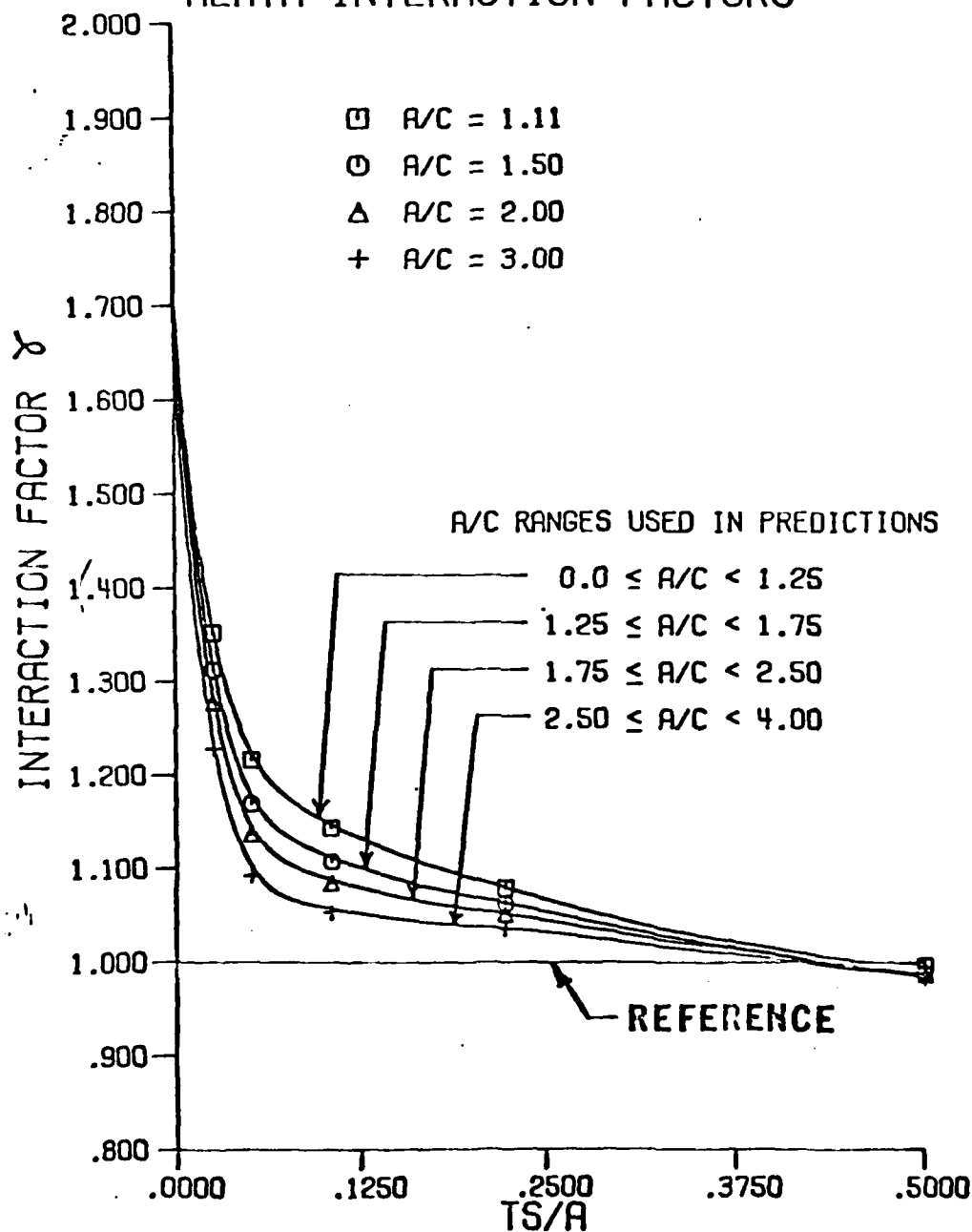obtain the dimensionless interaction factor γ given in Fig. 2. Here the

Fig. 2. Summary of the effect of crack spacing ts/a and crack shape a/c on stress intensity interaction factor γ at hole bore crack location.

increase in K at the point where the corner crack intersects the hole bore (locations 3 and 4 in Fig. 1c) is given as a function of dimensionless crack spacing ts/a and crack shape a/c. Note in Fig. 2 that as the cracks approach coalescence (ts/a < 0.3), K is increased significantly along the hole bore. In addition, flaw shape has a relatively minor effect on the increase in K. Since, Heath and Grandt showed that the stress intensity factor at free surface locations 2 and 5 is relatively unaffected by the approaching crack, no interaction was considered at those points, and the single crack Newman-Raju (1981) solutions were used to compute K there.

Thus, Equations 1 through 3 were solved in an iterative manner which allows the cracks to grow naturally. When the crack tips 3 and 4 touch, a single corner, surface, or through-the thickness flaw was assumed as appropriate, and the corresponding single crack K solution used to continue the analysis. Other possible combinations, such as penetration of surface crack locations 1 or 6 through a free surface to form corner flaws were also considered in the algorithm. Additional details are given by Tritsch (1983). Sample calculations obtained by this multi-degree-of-freedom analysis are compared with experimental results in the following section.

EXPERIMENTAL PROCEDURE

This section describes a set of experiments conducted with multi-cracked holes to provide initial evaluation of the predictive scheme. The double corner crack geometry given in Fig. 1c was considered here.

Test specimens were machined from a single sheet of polymethylmethacrylate (PMMA), a transparent polymer. The specimens were 25.4 cm (10.0 in.) long, 8.9 cm (3.5 in.) wide, 1.9 cm (0.75 in.) thick, and contained a central 0.95 cm (0.375 in.) diameter hole. The specimens were annealed to relieve possible residual stresses, and the ends were polished to transparency. Small notches were cut with a razor blade along the hole bore (on opposite sides of the plate thickness) to provide crack initiation sites. The specimens were then precracked in cyclic bending until fatigue cracks had completely surrounded the pre-notches.

Following precracking, grips were bonded to the ends of the specimens and a constant amplitude tensile load was applied at 2 Hz with a closed loop electrohydraulic fatigue machine. Strain gages were mounted to the front and back sides of the specimens to verify that uniform tension was applied without bending. A cutout in one end of the grips allowed a mirror to be placed at an angle over the transparent specimen end and provided optical access to the crack plane. Crack growth was recorded with a 35 mm camera, and the film strips measured to give crack dimensions as a function of applied load cycles. Additional experimental details are given by Perez (1983).

Fatigue crack growth curves for two specimens are given in Figs. 3 and 4. Here the experimental measurements are given by the data points defined in the legends on Figs. 3 and 4. Measurements are given for the four crack dimensions a1 and c1 (crack 1) and a2 and c2 (crack 2) prior to coalescence. Following link up, the surface dimensions c1 and c2 of the through-the-thickness flaw are also given.

The solid and dashed lines in Figs. 3 and 4 are predictions obtained by the numerical scheme discussed in the last section. Baseline fatigue crack growth data (da/dN versus ΔK) were obtained with additional through-cracked
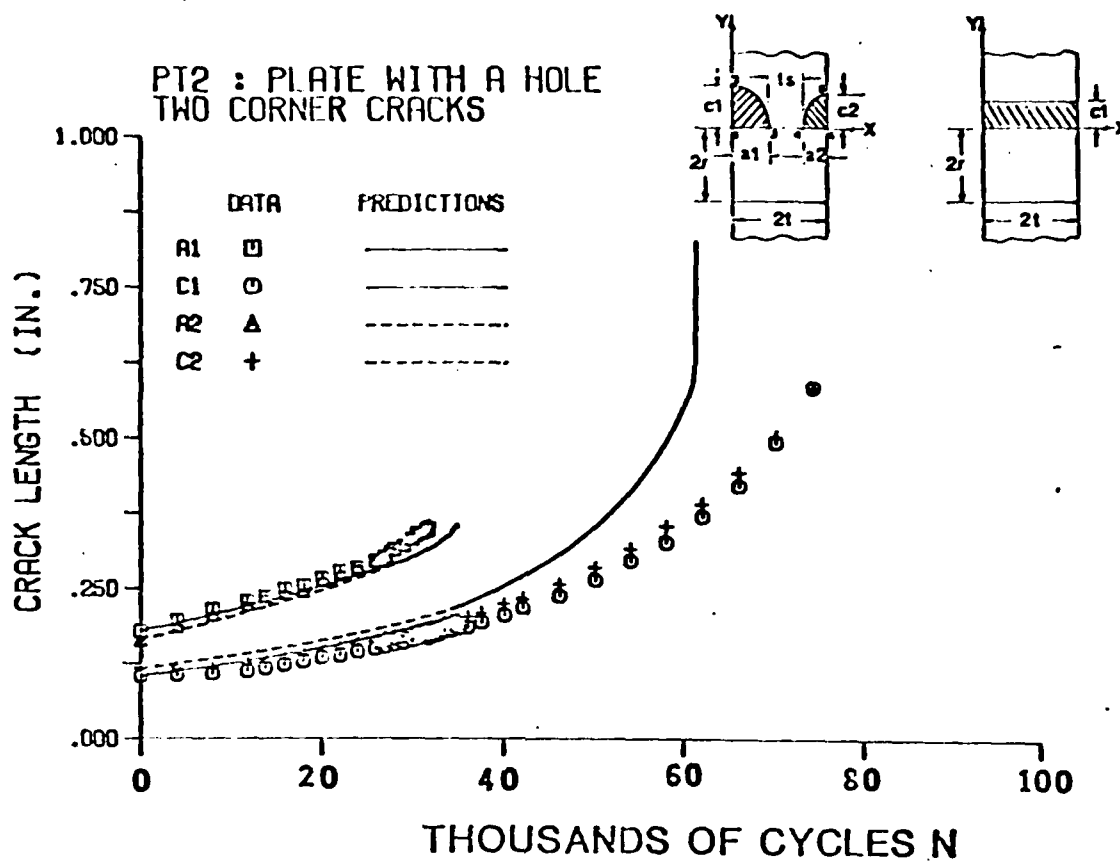
Fig. 3. Comparison of experimental and numerical results for growth of two corner cracks at open hole.
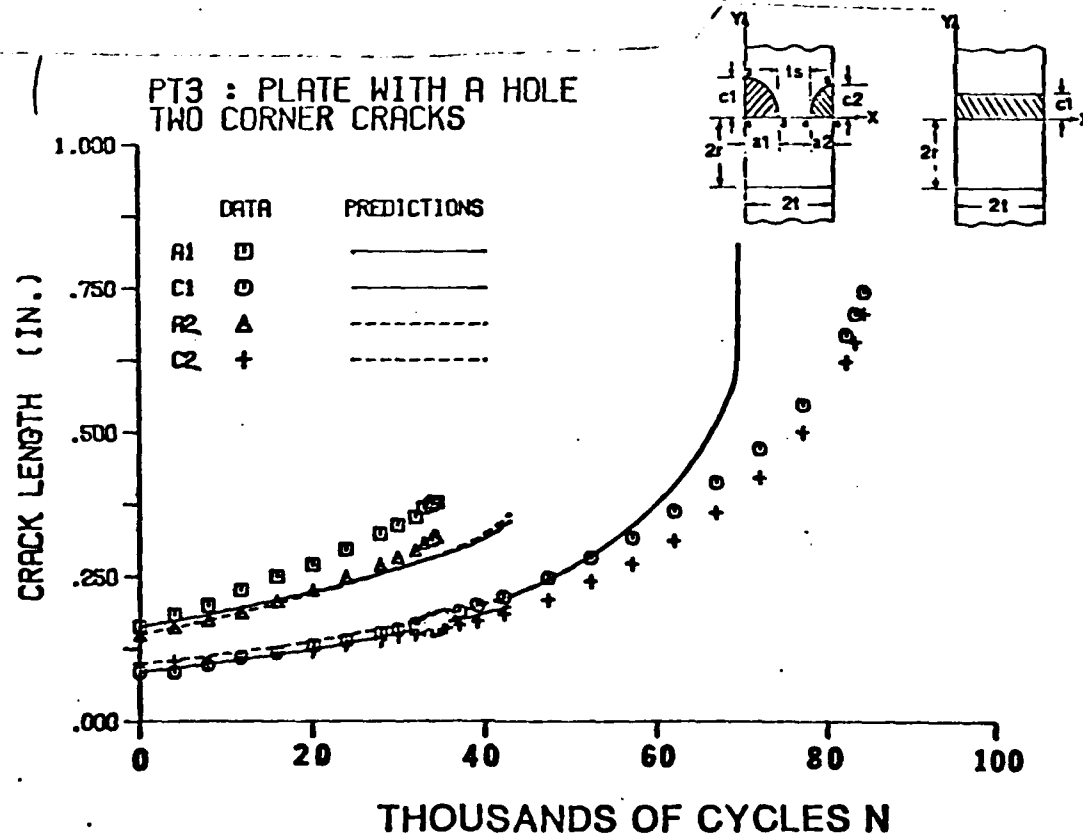

Fig. 4. Comparison of experimental and numerical results for growth of two corner cracks at open hole.

specimens obtained from the same sheet of PMMA and loaded at the same cyclic frequency. A simple power law was used to fit these baseline data and provided the crack growth model used for Eq. 3. Care was taken not to extrapolate the fatigue crack growth law for the baseline data beyond its limits of validity.

Note that the predictions of Figs. 3 and 4 generally agree quite well with the experimental data. In both cases, coalescence occurred slightly before the prediction, but actual fracture occurred shortly following the analysis. The latter result is more likely due to conservatism in the analysis scheme resulting from the fact that transition to a uniform through-the-thickness flaw was assumed to occur immediately following coalescence (joining of points 3 and 4). In actuality, a short period of time was required for the joined cracks to grow into a uniform front. More detailed measurements of the transition crack growth are given by Perez (1983).

CONCLUDING REMARKS

The objective of this paper has been to describe a procedure for predicting the lives of components which contain two or more adjacent cracks. A multi-degree of freedom model has been described for computing the initial growth, coalescence, and final extension of corner and surface cracks located along the bore of a hole in an open plate. Experiments described here with corner cracked holes in transparent polymer specimens gave excellent agreement with the predictive model. Similar predictions have been made by the authors for experiments in more conventional structural metals, and also show good agreement between experiment and analysis. (It is planned to describe those results in a separate paper.)

Although the present model is limited to two initial cracks, the procedure is readily extended to additional flaws. The stress intensity factor calcu-lations for interacting cracks, based on the single crack solutions given by Newman and Raju (1981) and modified by the crack interaction factor obtained by Heath and Grandt for symmetric corner cracks, worked well for the experiments which have been examined to date. It may be necessary to develop alternate interaction factors for crack combinations which differ greatly in size, as the Heath and Grandt result assumes symmetric flaws. In addition, cracks which initiate in different planes may need to be analyzed by an alternate procedure.

ACKNOWLEDGMENTS

REFERENCES

Heath, B.J., and Grandt, A.F., "Stress-Intensity Factors for Coalescing and Single Corner Flaws Along a Hole Bore in a Plate," _Engineering Fracture Mechanics_, Volume 19, No. 4, 1984, pp. 665-673.

Newman, J.C. and Raju, I.S., "Stress-Intensity Factor Equations for Cracks in Three-Dimensional Finite Bodies," NASA Technical Memorandum 83200, NASA Langley Research Center, Hampton, Virginia 23665, August 1981.

Perez, R., "Initiation, Growth, and Coalescence of Fatigue Cracks," M.S. Thesis, School of Aeronautics and Astronautics, Purdue University, W. Lafayette, IN 47907, August 1983.

Tritsch, D.E., "Prediction of Fatigue Crack Lives and Shapes," M.S. Thesis, School of Aeronautics and Astronautics, Purdue University, W. Lafayette, IN 47907, August 1983.

AN EXPERIMENTAL AND NUMERICAL INVESTIGATION OF THE
GROWTH AND COALESCENCE OF MULTIPLE FATIGUE CRACKS AT NOTCHES

by

A. F. Grandt, Jr. [1]

A. B. Thakker [2]

D. E. Tritsch [3]

ABSTRACT

The objective of this paper is to describe results of an
experimental and numerical study concerned with predicting the
growth and coalescence of multiple fatigue cracks. Naturally
occuring fatigue cracks frequently initiate at multiple sites
near stress concentrations. Individual cracks then grow by
cyclic loading, until eventually two or more adjacent cracks link
up into a single, dominant flaw which grows to final failure.
Figure 1 shows schematic examples of various surface and corner
crack combinations located at the bore of a notch. The current
paper describes a life prediction scheme for computing the total
life of such multiply cracked notches.

The fatigue crack growth algorithm is based on conventional
linear elastic fracture mechanics concepts. Stress intensity
factors are computed at various points along the crack tip (such

[1,3] Professor and Graduate Assistant, respectively, School of
      Aeronautics and Astronautics, Purdue University, W.
      Lafayette, IN 47907.

[2] Rolls Royce, Inc., 1915 Phoenix Blvd., Atlanta, GA 30349.

as points 1 to 6 in Fig. 1a). The fatigue crack growth law for the component material is then used to compute an increment of crack growth at these flaw locations. The crack shape then changes, and the procedure is repeated in an iterative fashion until the flaws coalesce, penetrate a free surface, or cause fracture. The cycles required for growth of the multiple cracks, and the resulting single coalesced flaw, are summed as the iteration proceeds to give total life.

The stress intensity factors are based on solutions by Newman and Raju (1) for single surface and corner cracks located at holes. These single crack results are then modified by an "interaction factor" obtained from a stress intensity factor solution for multiple corner cracks (2). In this manner, the influence of the adjacent flaw on the stress intensity factor at crack tip locations 3 and 4 is determined (see Fig. 1a). Once crack tips 3 and 4 join, a single surface or corner crack is assumed, and the appropriate K solution for the single flaw (1) is employed. If the crack continues to grow, and becomes a through-the-thickness flaw, then the appropriate through-crack K solution is used. Additional modifications to consider semicircular edge notches are described in the paper.

A set of experiments with multiply flawed specimens were conducted to evaluate the multiple degree-of-freedom life prediction analysis outlined above. Waspalloy and titanium specimens were machined to the configuration shown in Fig. 2. Surface cracks were initiated at small elox starter slots located along

the bore of one of the semicircular edge notches. The specimens were then cycled to failure under constant amplitude loading applied perpendicular to the crack plane. The fracture surfaces were periodically marked by heat tinting procedures (the test temperature was briefly changed) so that the crack dimensions could be determined following final specimen fracture.

Figure 3 compares experimental and numerical results for a typical test. The open symbols are measures of crack dimensions obtained by the heat tinting technique, while the solid lines represent predictions by the numerical analysis. The results of approximately one dozen tests are presented, and show that, in general, the analysis scheme provides an excellent estimate for the initial growth of the multiple cracks, their eventual coalescence into a single crack, and growth of the final flaw.

REFERENCES

1. J.C. Newman, Jr. and I.S. Raju, "Stress-Intensity Factor Equations for Cracks in Three-Dimensional Finite Bodies," NASA Technical Memorandum 83200, NASA Langley Research Center, August 1981.

2. B.J. Heath and A. F. Grandt, Jr., "Stress Intensity Factors for Coalescing and Single Corner Flaws along a Hole Bore in a Plate," Engineering Fracture Mechanics, (in press).
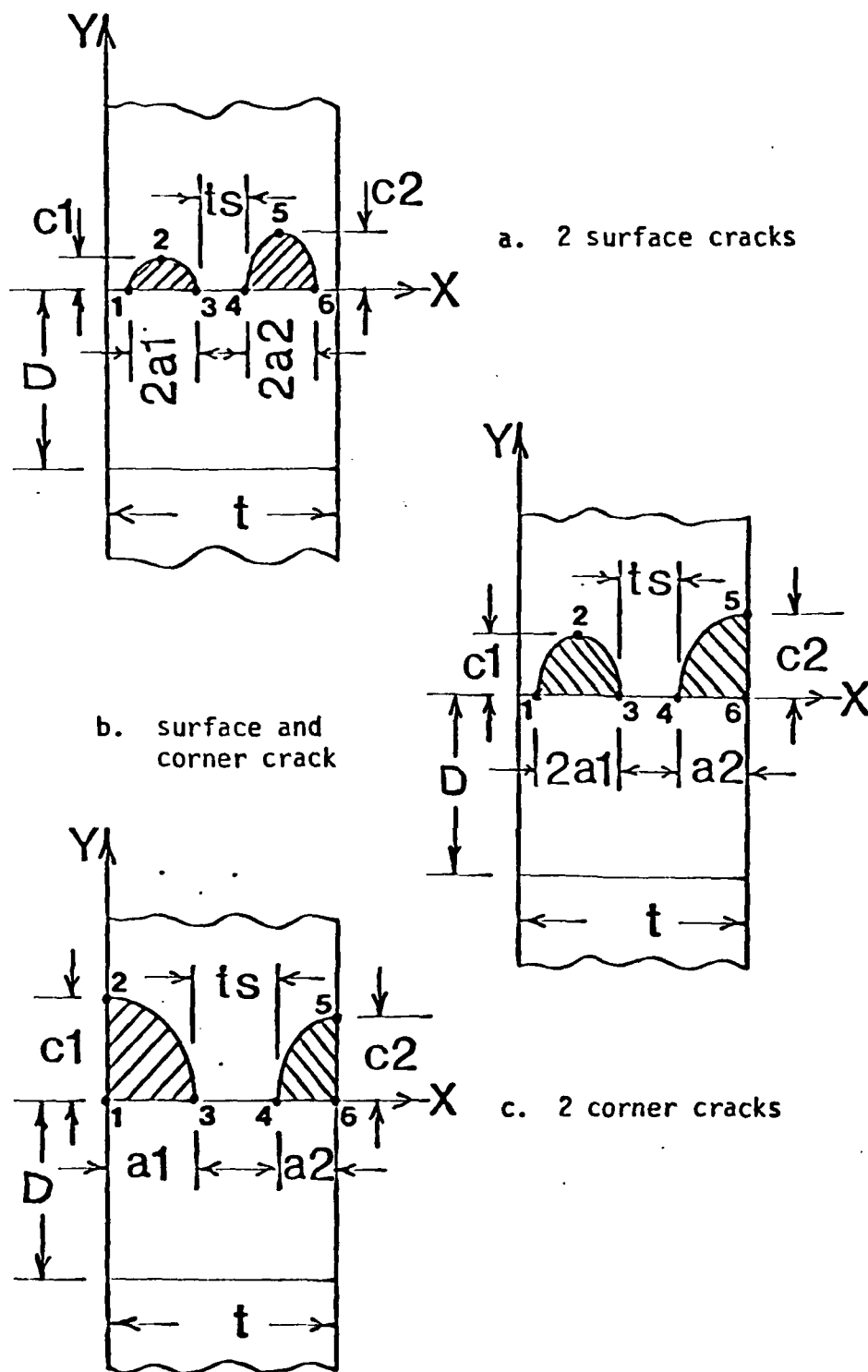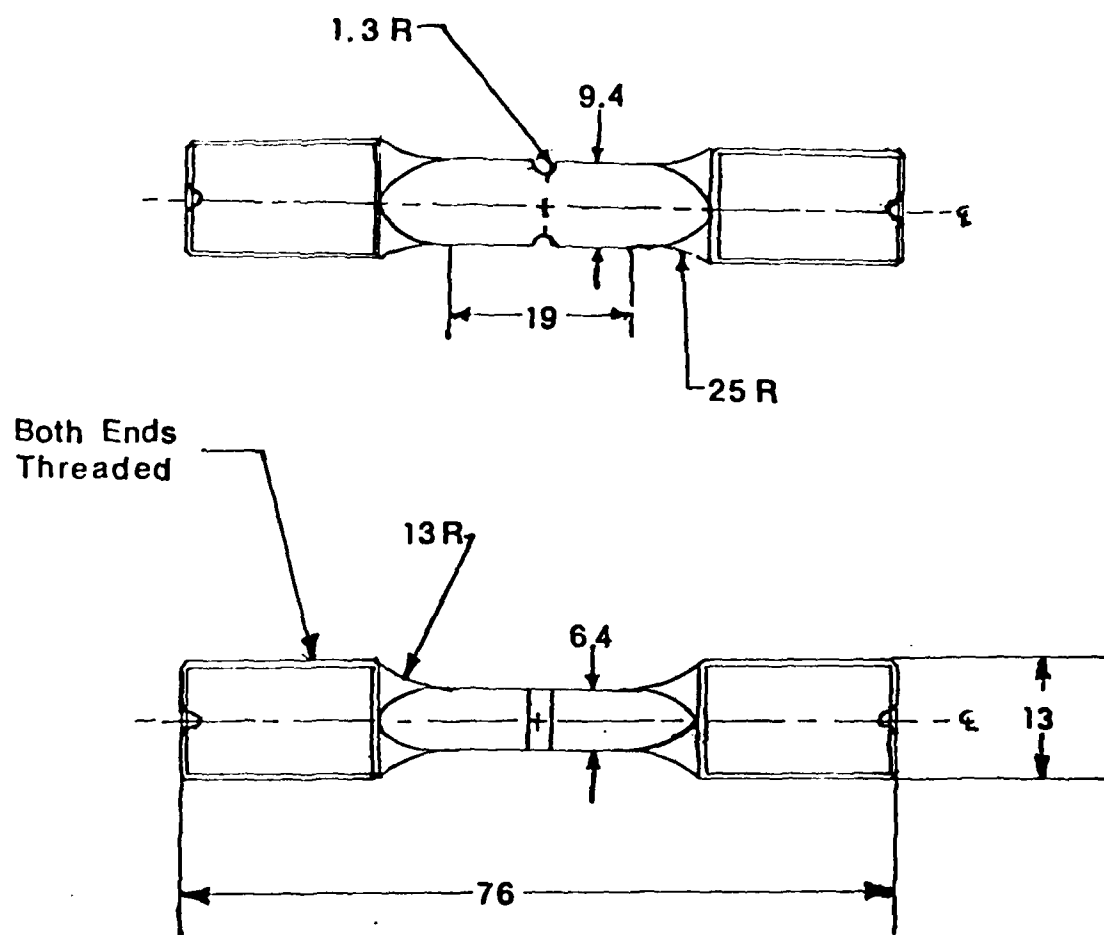
Figure 1 Schematic of multiple cracks located along bore of a hole in a large plate. Hole diameter is D, plate thickness is t, and remote tensile stress is applied in z direction.

All dimensions are in mm

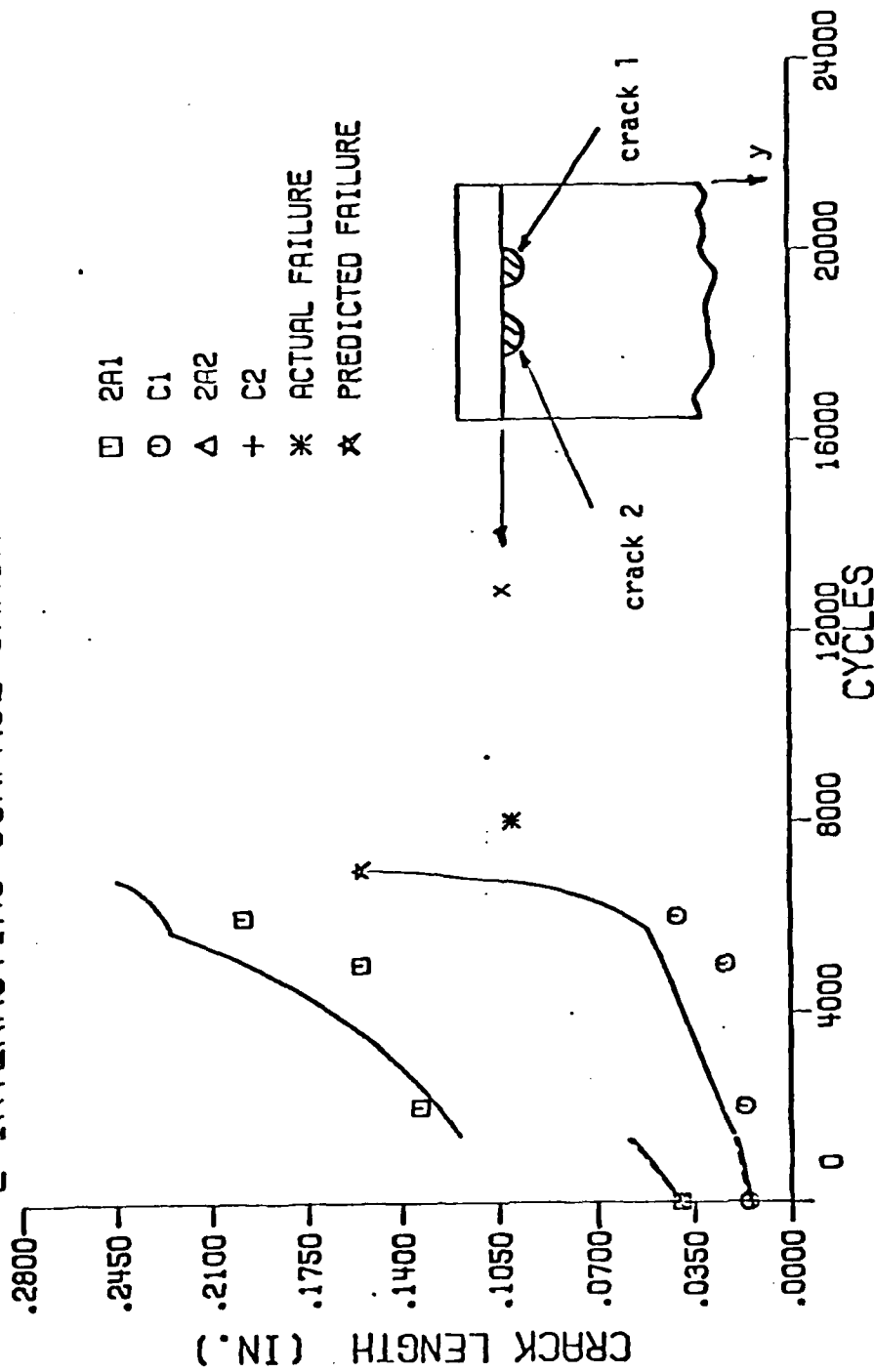Figure 2   Drawing of test specimen showing specimen dimensions and location of two semicircular edge notches.

Figure 3 Comparison of predicted and experimental growth and coalescence of two surface cracks at semicircular notch in Waspaloy specimen

END

FILMED

5-85

DTIC